NASA TECHNICAL
MEMORANDUM

NASA TM X-62,015

NASA TM X-62,015

HYPERVELOCITY OXIDATION TESTS OF THORIA DISPERSED NICKEL CHROMIUM ALLOYS

Frank J. Centolanzi

Ames Research Center
Moffett Field, Calif. 94035

February 11, 1971

HYPERVELOCITY OXIDATION TESTS OF

THORIA DISPERSED NICKEL CHROMIUM ALLOYS

By Frank J. Centolanzi

SUMMARY

This report describes hypervelocity oxidation tests of thoria dispersed nickel chromium alloys which are being considered for use on the Space Shuttle Vehicle. Measurements of mass loss in both stagnation and wedge flows are presented, together with estimates of emissivity derived from radiometric measurements. The results of detailed metallurgical examination of the specimens conducted by the Lewis Research Center are also shown.

The results show that thoria dispersed nichrome (TD-NiCr) loses weight steadily with time in a hypervelocity environment. This loss of weight results in internal depletion of chromium accompanied by porosity. A modified alloy, containing aluminum and yttrium (TD-NiCrAlY), has superior oxidation resistance. Its emissivity, however, is considerably lower.

INTRODUCTION

During the past year there has been considerable effort directed toward the development of thermal protection systems (TPS) for reusable space shuttle vehicles. One type of TPS involves the use of radiation cooling to accomodate the convective heating which is generated during re-entry. With this system, the skin consists of a high temperature, high emittance material backed by a high temperature insulator. There are many candidate materials, both metallic and non-metallic, for this type of TPS. One of the metallic materials receiving widespread attention is the dispersion strengthened alloy Ni-20Cr-2ThO_2, more commonly called TD-nichrome (TD-NiCr).

As a candidate for a reusable heat shield material, TD-NiCr must resist oxidation and, at the same time, retain its inherently high strength at temperature. Early experiments in static or slowly moving air (Refs. 1, 2 and 3) indicated nickel-chromium alloys to be highly resistant to oxidation. Samples tested in that environment tended to show a slow gain of weight. More recently, tests have been made at high flow rates in combustion facilities (Ref. 4). In sharp contrast to the static tests, the samples tested in a flowing environment showed a weight loss with time, an indication that flow was an important variable governing the oxidation of TD-NiCr.

In order to evaluate this material as a potential heat shield candidate for the space shuttle vehicle, it was apparent that tests at conditions which more closely approximate the space shuttle entry environment were needed. A test program was initiated with the following objectives:

1. To obtain hypervelocity oxidation data in the anticipated temperature range of the space shuttle vehicle (1800° - 2200°F) supplemented with accurate measurements of mass loss vs time. The mass loss measurements are the unique feature of this investigation.

2. To obtain data on the effect of surface pressure on the oxidation rates.

3. To provide data at various enthalpy and shear levels using two types of flows:

   a. A stagnation flow where the air impinges on the sample at right angles to the planar surface.

   b. A shear type flow where the sample is imbedded in the surface of a wedge having a locally supersonic boundary layer.

4. To obtain radiometric data to provide an estimate of the emissivity of this material at high temperatures.

5. To provide early oxidation data on a modification of TD-NiCr containing aluminum and yttrium which may be used as an alternate alloy in the event TD-NiCr was unsatisfactory.

The post-test metallography for this investigation was done at the Lewis Research Center with the kind cooperation of Dr. H. B. Probst, and Mr. C. E. Lowell. These results are also described in this paper.

After the completion of these experiments, Goldstein (Reference 5) developed an analytical model describing the hypersonic ablation of thoria dispersed nickel chromium alloys. Comparison of some of these data with theoretical predictions are presented in his paper.

SPECIMENS AND SUPPORTS

Two dispersion strengthened alloys manufactured by the Fansteel Corporation were investigated. The first, an alloy containing Ni-20Cr-2ThO_2, is considered one of the prime candidates for use on the shuttle vehicle. The second, a proprietary alloy containing Ni-16Cr-2ThO_2 with addition of aluminum and yttrium is considered an alternate material because of its higher oxidation resistance in static tests, but is considerably more difficult to fabricate.

The stagnation region and wedge test supports are shown in Figure 1. Both supports were constructed to accommodate one-inch diameter disk-shaped samples. The initial materials tested were nominally .012 inches thick. The test samples were insulated from the rear by fused silica cylinders and centered with four stainless steel screws to avoid contact with the lower temperature surfaces of the support. A platinum--platinum,13 percent rhodium thermocouple was spot welded to the back of each specimen. Before exposure to the hypervelocity stream the samples were pre-oxidized at 1900°F in atmospheric air for 1/2 hour to increase their emissivity.

FACILITY AND TESTS

The tests were conducted in the Aerodynamic Test Facility of the Ames Thermal Protection Branch. This facility is designed to accommodate a variety of arc heaters and nozzle combinations thereby providing a wide range of test conditions. The facility and arc-heater arrangement is shown in Figure 2. The arc heater used for these tests was a Linde Model 4001. Coarse enthalpy control was accomplished by injection of cold air through a mixing ring downstream of the heater. Variation of arc current provided the fine enthalpy control. The supports are shown mounted on a traversing mechanism in the test chamber in Figure 3. Also shown are the hemispherical calorimeters and pitot probes which furnished a measure of the stream conditions for each run.

The installation of the Thermadot TD-6BT Radiation Thermometer is shown schematically for the stagnation tests in Figure 4. A similar arrangement was used for the wedge tests.

The actual material temperature of the test sample was measured by a thermocouple spot-welded to the back surface of the specimen. The emissivity at which the radiometer must be set in order to read the true temperature provides an estimate of the emissivity of the test material.

A typical test cycle consisted of starting the arc-jet and establishing test conditions. The sample holder was then inserted into the stream. Temperatures were monitored with the thermocouple and a digital voltmeter. Continuous recordings of temperatures and pressures were made on oscillograph tapes during the run. After 1800 seconds in the stream the samples were withdrawn and the calorimeters inserted. This procedure was repeated until the desired number of simulated entry cycles was reached. Photographs taken during typical runs are shown in Figure 5. The test conditions for the stagnation and wedge tests are tabulated below.

Stagnation Tests

Material and Specimen No.	Nominal Temperature, °F	Nominal Surface Pressure, Torr	Enthalpy, Btu/Lb	Total Number of 1800sec cycles
TD-NiCr-1	1800	15	1900	50
TD-NiCr-2	2200	15	2900	50
TD-NiCr-8	2200	30	2100	34
TD-NiCiAlY-2	2200	15	2900	40

Wedge Tests

Material	Nominal Temperature, °F		Nominal Surface Pressure, Torr	Enthalpy, Btu/Lb	Total Number of 1800sec cycles
	Front Specimen No.6	Rear Specimen No.7			
TD-NiCr	2200	2000	15	5000	28

Typical post run photographs of the stagnation test and wedge test are shown in Figure 6. After the tests were completed all the specimens were photographed and are shown in Figure 7.

RESULTS

Weight Changes--Stagnation Tests

The weight change data for TD-NiCr at 15 torr surface pressure and temperatures of 1800°F and 2200°F are shown in Figure 8. At 2200°F the specimen loses weight at a rate which is almost linear with time after the first several cycles. These results are in sharp contrast to the static tests reported in References 1, 2 and 3 which show weight increases

with time typical of oxidation where a protective layer of increasing thickness is formed. The mass losses at 1800°F were small compared to those at 2200°F. The oxide on the surface of the specimen tested at 2200°F was greenish-yellow compared to the dark colored oxide reported for the static tests. The oxide layer for the specimen tested at 1800°F was brownish in appearance. It was later learned that this was a result of stream contamination with copper resulting from erosion of the arc-heater electrodes. The affect of copper contamination on the oxidation mechanism of this alloy is not known.

The affect of pressure on the rate of mass loss is shown in Figure 9. Increase of surface pressure from 15 to 30 torr resulted in mass losses which were about 25 percent higher.

Mass loss measurements of TD-NiCr compared with the modified alloy containing additions of aluminum and yttrium (TD-NiCrAlY) are shown in Figure 10. This alloy also loses weight, but at a rate much lower than TD-NiCr, probably because of the formation of a stable oxide of alumina at the surface.

Weight Changes--Wedge Tests

The mass loss data for the wedge test is shown in Figure 11. Because of the limitations and sample support complexity, the test samples were only weighed twice, before and after the completion of 28 cycles, where the tests were prematurely terminated because of a failure in the steam ejector plant which provides the vacuum for the test facility. The temperature of the forward test sample was maintained at 2200°F throughout the test, while that of rear sample was about 2000°F, due to the heating rate decreasing as a function of distance along the wedge. The mass losses measured in the wedge test were greater than the corresponding mass losses in the stagnation tests by about 20 percent. The mass loss at 2000°F was less than half that at 2200°F.

Radiometric Data

Some typical temperature distributions over the face of the test samples taken with the radiometer are shown in Figure 12. The temperatures are essentially constant since the aerodynamic heat transfer rates are essentially constant in the central region of a blunt-faced cylinder.

The temperatures measured by the thermocouple and radiometer furnish a measure of the sample surface emissivity. When the temperatures measured by the thermocouple and the radiometer are equal, the emissivity of the test sample may be determined by the expression

$$\varepsilon_{sample} = \frac{\varepsilon_{set}}{\varepsilon_{window}}$$

where ε_{set} is the ε_{window} emissivity setting on the calibrated dial of the radiometer. The emissivity of the window for these tests was determined to be about 0.77 ± .05 by direct calibration using a black body source of known temperature. The measured emissivity results are tabulated below.

Material	Temperature, °F	ε_{Set}	ε_{Sample}
TD-NiCr	2200°F	0.67	0.85±.05
TD-NiCr	1800°F	0.67	0.85±.05
TD-NiCrAlY	2200°F	0.55	0.70±.05

There is a considerable difference between the emissivity of TD-NiCr and TD-NiCrAlY. This difference, which probably results from different oxides being formed at the surface during the test exposures, could result in significantly different radiative equilibrium temperatures for the two materials at a given heat flux. There are several possible sources of error in attempting to make in-situ measurements of emissivity. One of these is reflected energy from the arc heater to the radiometer via the model surface. The magnitude of this error is not known. In-situ measurements of emissivity should be coupled with post oxidation measurements using standard techniques.

Metallography

The metallurgical examination of the test samples was conducted at the Lewis Research Center with the kind cooperation of Dr. H. B. Probst and Mr. C. E. Lowell. The results are described in the following sections and summarized at the end of this section in Table I.

Scale Identification

The oxide scale on the front and back surfaces of the samples was identified by X-Ray diffraction. The results are shown in the following table:

SUMMARY OF SCALE IDENTIFICATION

Material	Type of Test	Temperature °F	Surface Pressure, Torr	Number of 1800 sec. Cycles	Front Side		Back Side	
					Phase	Relative* Intensity	Phase	Relative* Intensity
TD-NiCr	Stagnation	2200	15	50	NiO Cr_2O_3 $NiCr_2O_4$	Strong Medium Medium	NiO Cr_2O_3 $NiCr_2O_4$	Strong Medium Very Weak
TD-NiCr	Stagnation	1800	15	50	$Cu_2Cr_2O_4$ NiO	Very Strong Strong	Cr_2O_3 NiO	Strong Weak
TD-NiCr	Stagnation	2200	30	34	NiO Cr_2O_3 $NiCr_2O_4$	Very Strong Medium to Weak Medium to weak	-------	--------
TD-NiCr	Wedge	2200	15	28	NiO Cr_2O_3 $NiCr_2O_4$	About the same intensity	------	--------
TD-NiCr	Wedge	2000	15	28	NiO Cr_2O_3 $NiCr_2O_4$	About the same intensity	------	--------
TD-NiCrAlY	Stagnation	2200	15	40	Al_2O_3	----------	------	--------

* Intensity is proportional to concentration.

The results showed a variety of oxides being formed at the surface during hypervelocity oxidation. For the TD-NiCr the oxides are NiO, Cr_2O_3, and $NiCr_2O_4$. For the alloy TD-NiCrAlY the oxide formed at the surface is Al_2O_3. This stable oxide, which is relatively impervious, is responsible for the lower mass losses observed.

The sample of TD-NiCr tested at 1800°F showed large amounts of copper present in the oxide. This accounts for the brown color observed on this sample during the tests. The source of copper is the erosion of the electrodes of the arc heater which are constructed of a copper-silver alloy. These electrodes are gradually consumed during the arc heater operation. The effect of this copper contamination on the oxidation mechanism of the material is not known. There was no evidence of copper on the samples tested at higher temperatures. Apparently, copper or copper oxide which condenses on the samples at 1800°F does not condense at 2200°F. Because of this, testing in arc heaters of this type at the lower temperatures could give erroneous results.

Microstructures

Cross sections of all the test samples are shown in Figure 13 through 17. The samples mounted in the wedge support were sectioned along a plane parallel to the gas flow direction. There are several things which are evident from inspection of the micrographs:

1. For TD-NiCr the oxidation is generally more severe on the front side than on the back side which is protected from the flowing air.

2. All the TD-NiCr samples exhibit porosity (the dark globules in the micrographs) after exposure to hypervelocity air flow. The degree of porosity varies with temperature, time of exposure, and possibly pressure.

3. In contrast to the TD-NiCr, the alloy TD-NiCrAlY showed no porosity after 40 cycles of 1800 seconds duration.

Metal Loss

Measurements of the remaining metal thickness were made along the cross section of each sample before etching and the results are presented in Figure 18. The measurements were made using a filar eyepiece. Due to the irregularity of the scale-metal interface, measurement and interpretation of the thickness was difficult in some cases. By subtracting these measurements from the original thicknesses the metal losses were obtained. In general, the metal loss is not particularly uniform over the cross section of the samples. There are several reasons for the locally high metal loss for some of the samples. Near the center, where the thermocouple is located, the spot welding operation could cause locally high losses. In some cases, locally high metal losses were observed near the edges of the sample. This could result from local scale cracking, or a section being taken near one of the four support tabs (which were spot welded). For the case of the TD-NiCrAlY, the high edge loss was the result of locally severe aerodynamic heating due to a slight warping of the sample.

The metal loss for TD-NiCr increases with temperature, time of exposure, and pressure. The shear provided by the supersonic laminar boundary layer of the wedge tests does not appear to be a significant factor. The metal loss for the alloy TD-NiCrAlY was lower than any of the TD-NiCr alloys tested.

Internal Chemistry

The distribution of Ni, Cr, Th, and Al below the surfaces exposed to air flow was determined by electron microprobe and the results are shown in Figure 19. Several conclusions can be made from inspection of these results:

1. For TD-NiCr, chrome depletion beneath the surface results from exposure to hypervelocity gas flow. The magnitude of the depletion is dependent upon temperature, time of exposure, and probably pressure. In contrast, TD-NiCrAlY shows no measurable depletion of chromium.

2. For TD-NiCr, chromium and nickel are important components in the scale. TD-NiCrAlY has mainly alumina in the scale.

3. The depletion of chromium explains the porosity observed in the TD-NiCr specimens.

Lattice parameters of the solid solutions at the surface obtained by X-Ray diffraction were used to estimate the chromium content at the surface. These values were converted to weight percentages using calibration curves available in the literature. This information is summarized below:

Sample	A_o (Angstroms)	Weight Percentage, Cr
TD-NiCr-1	3.540	16
TD-NiCr-2	3.536	11
TD-NiCr-6	3.542	16
TD-NiCr-7	3.544	17
TD-NiCr-8	3.536	11

The combined qualitative information from the electron microprobe and the semi-quantitative values of the lattice parameters suggest that the overall content of Cr in specimens TD-NiCr-2 and TD-NiCr-8 is significantly less than the starting value of 20 percent. A direct measure of the chromium remaining in samples TD-NiCr-1 and TD-NiCr-2 was made using wet chemistry techniques. The amount of chromium remaining was found to be 19.6 and 15.0 percent for each sample, respectively.

CONCLUDING REMARKS

1. In sharp contrast to static test results, TD-NiCr loses weight steadily with time in a hypervelocity environment. As for all mass transport processes, the mass losses are dependent upon temperature, time, pressure, flight enthalpy, and material properties. A modified alloy, TD-NiCrAlY, loses considerably less weight because a protective oxide (alumina) is formed at the surface.

2. In-situ measurements of emissivity indicate TD-NiCr to have a value of about 0.85 $\pm$ .05 at 2200°F. The TD-NiCrAlY emissivity is considerably lower, about 0.70 $\pm$ .05.

3. Oxide scales formed on TD-NiCr are primarily NiO, Cr_2O_3, and $NiCr_2O_4$. A modified alloy, TD-NiCrAlY, forms mainly Al_2O_3.

4. In arc-jet tests, contamination from the copper electrodes can occur at lower temperatures (1800°F). Interpretation of results in this case is difficult.

5. After long exposure to hypervelocity air TD-NiCr suffers internal depletion of chromium. This depletion is accompanied by internal porosity which is concentrated near the surface of exposure. No depletion of chromium or internal porosity was observed for the alloy TD-NiCrAlY.

6. Metal loss for TD-NiCr depends upon temperature, time of exposure and pressure. The metal loss for TD-NiCrAlY is less than that for TD-NiCr because of a stable oxide of alumina which is formed at the surface.

7. The combined effects of porosity, chrome depletion, and metal loss would be expected to reduce the strength of TD-NiCr. The magnitude of this reduction is not known.

8. Some of these data have been compared with a recently developed analytical model by Goldstein of Ames Research Center. These results are presented in Reference 5. The theoretical predictions and the data are in good agreement.

REFERENCES

1. Gulbransen, E. A. and Andrew, K. F.: Oxidation Studies of the Nickel-Chromium and Nickel-Chromium-Aluminum Heater Alloys. Journal of the Electrochemical Society, Vol. 106, No. 11, pp 941-948, November 1959.

2. Gulbransen, E. A. and Andrew, K. F.: Rate of Oxidation of Three Nickel-Chromium Heater Alloys Between 500° and 900°C. Journal of the Electrochemical Society, Vol. 101, No. 4, pp. 163-170, April 1951.

3. Birks, N. and Rickert, H.: The Oxidation Mechanism of Some Nickel-Chromium Alloys. Journal of the Institute of Metals, Vol. 91, 1962.

4. Johnston, R. and Ashbrook, R. L.: Oxidation and Thermal Fatigue Cracking of Nickel and Cobalt-Base Alloys in a High Velocity Gas Stream. NASA TN D-5376, August 1969.

5. Goldstein, Howard E.: An Analytical Model for Hypersonic Ablation of Thoria Dispersed Nickel Chromium Alloy. Paper presented at AIAA 9th Aerospace Sciences Meeting, New York, New York, January 25-27, 1971. Also available as SSPD-23.

TABLE I

SUMMARY OF METALLOGRAPHIC RESULTS

Material and Identification Number	Temp. °F	Pressure TORR	Type of Test	Number of 1800 sec. Cycles	Total Time At Temperature Hours	Estimated Average Metal Loss Mils	Porosity	Depth of Cr Depletion From Metal/Scale Interface Mils	Weight % Cr At Surface, From Lattice Parameters
TD-NiCr-1	1800	15	Stagnation	50	25	1.4	Restricted to surface	1	16
TD-NiCr-2	2200	15	Stagnation	50	25	2.0	Severe	>6 depleted to center-line of sample	11
TD-NiCr-6	2200	15	Wedge	28	14	2.0	Moderate (less than TD-NiCr-2)	3	16
TD-NiCr-7	2000	15	Wedge	28	14	1.2	Mild	2	17
TD-NiCr-8	2200	30	Stagnation	34	17	2.5	Severe	4	11
TD-NiCrAlY	2200	15	Stagnation	40	20	0.8	None	Zero	--

National Aeronautics and Space Administration
Ames Research Center
Moffett Field, Calif.

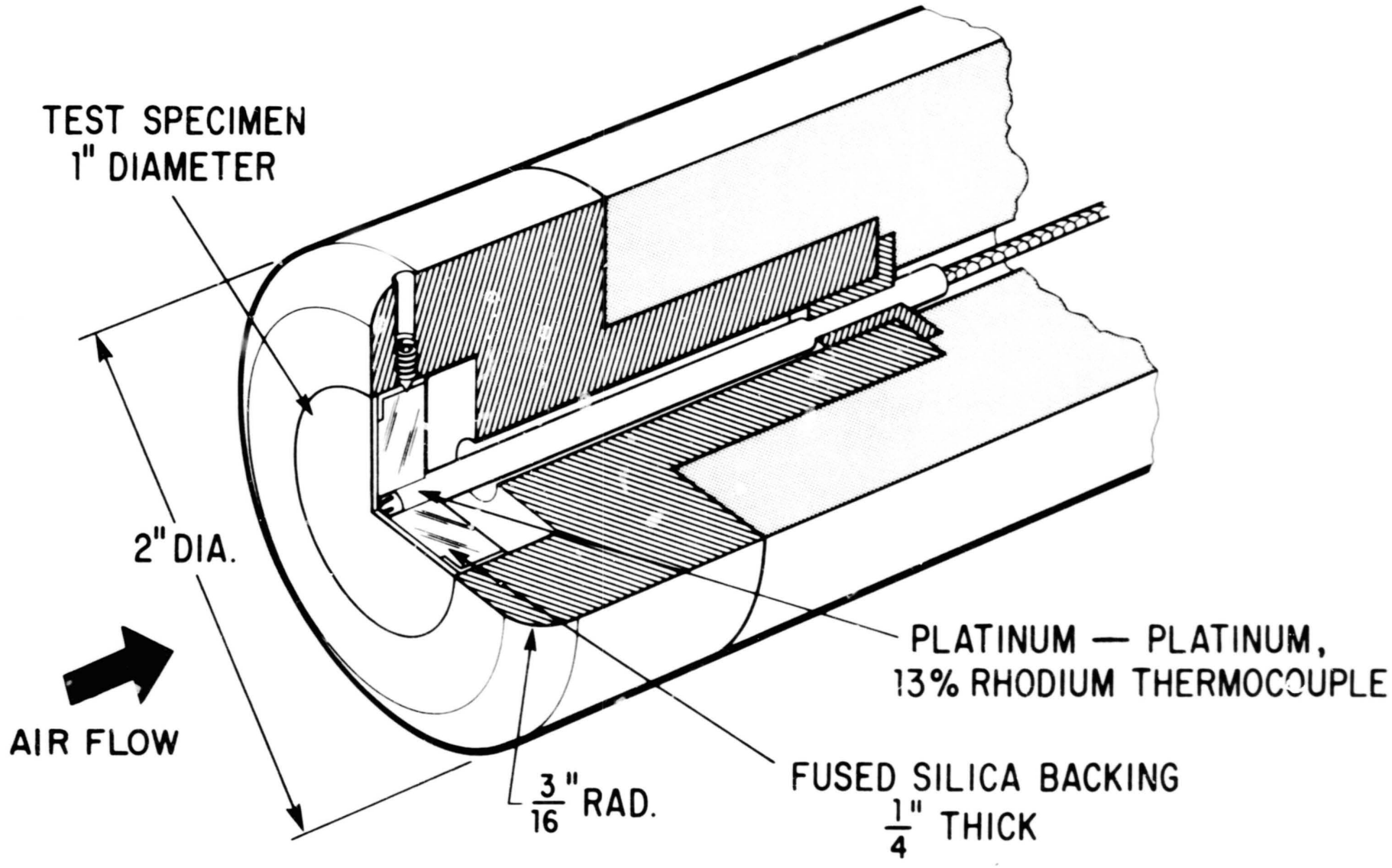

(a) Stagnation test support.

Figure 1.- Sample supports for arc-jet tests.

National Aeronautics and Space Administration
Ames Research Center
Moffett Field, Calif.

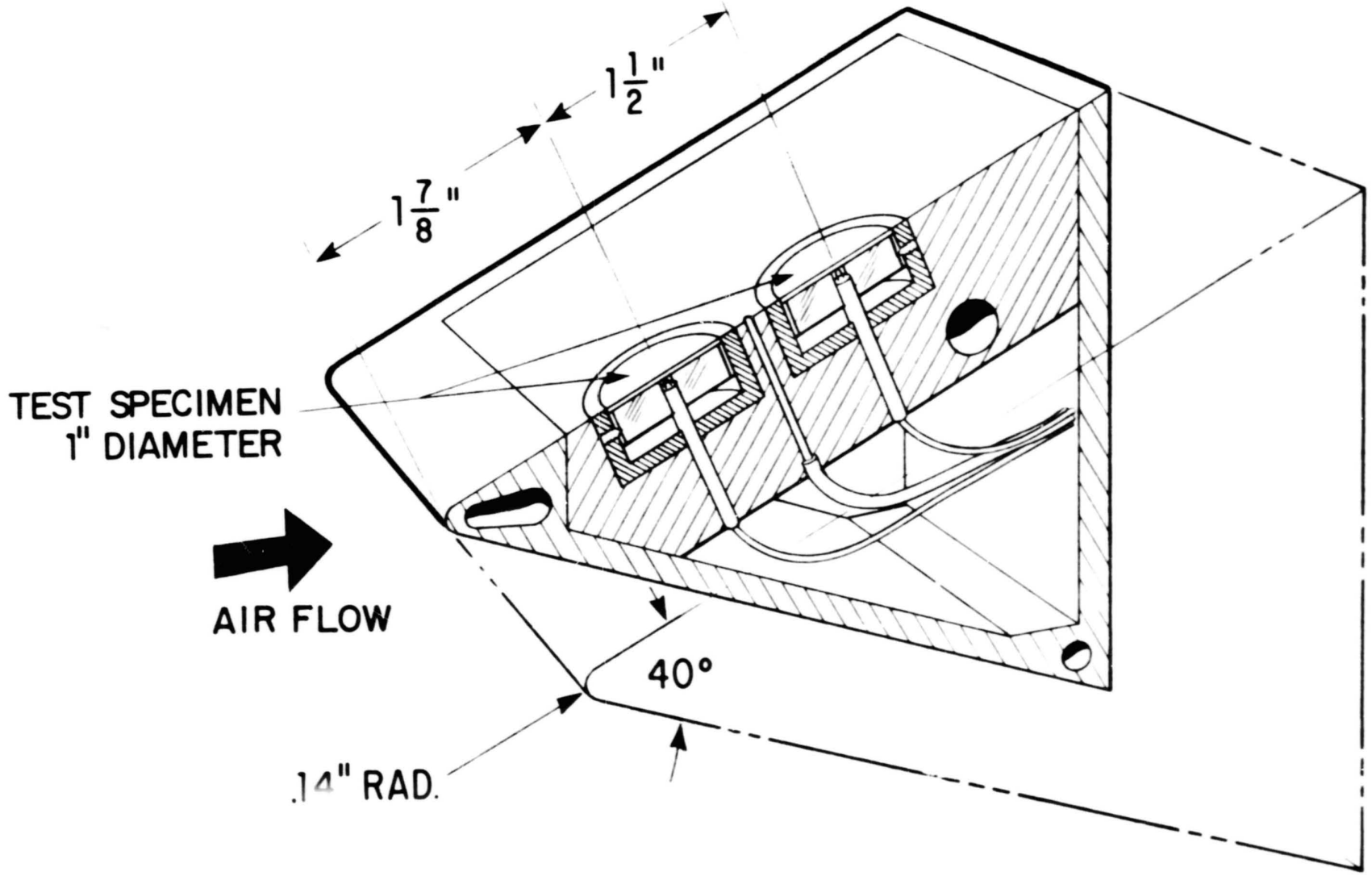

(b) Wedge test support.

Figure 1.- Concluded.

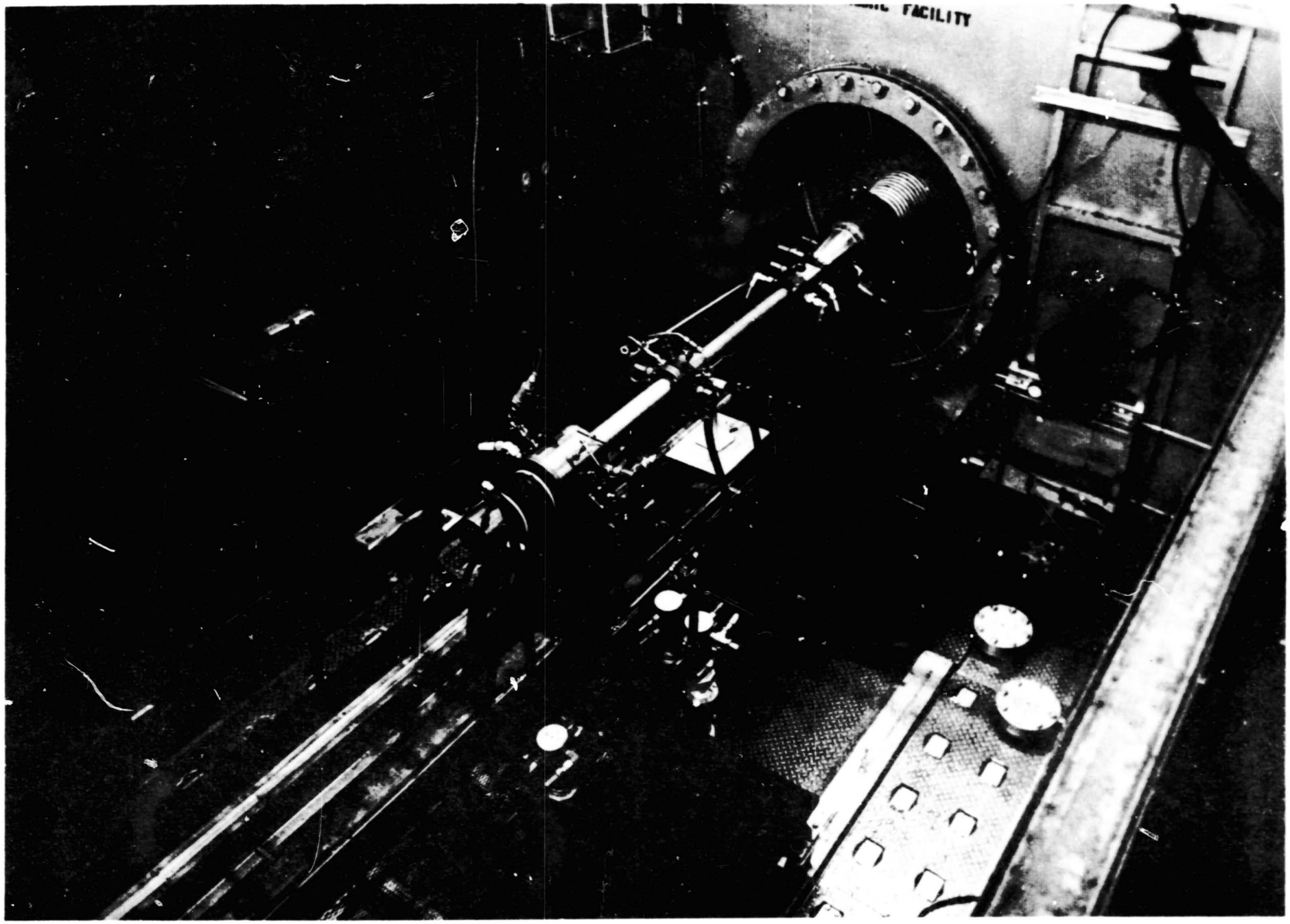

Figure 2.- Test facility and arc heater setup.

NATIONAL AERONAUTICS AND SPACE ADMINISTRATION
AMES RESEARCH CENTER, MOFFETT FIELD, CALIFORNIA

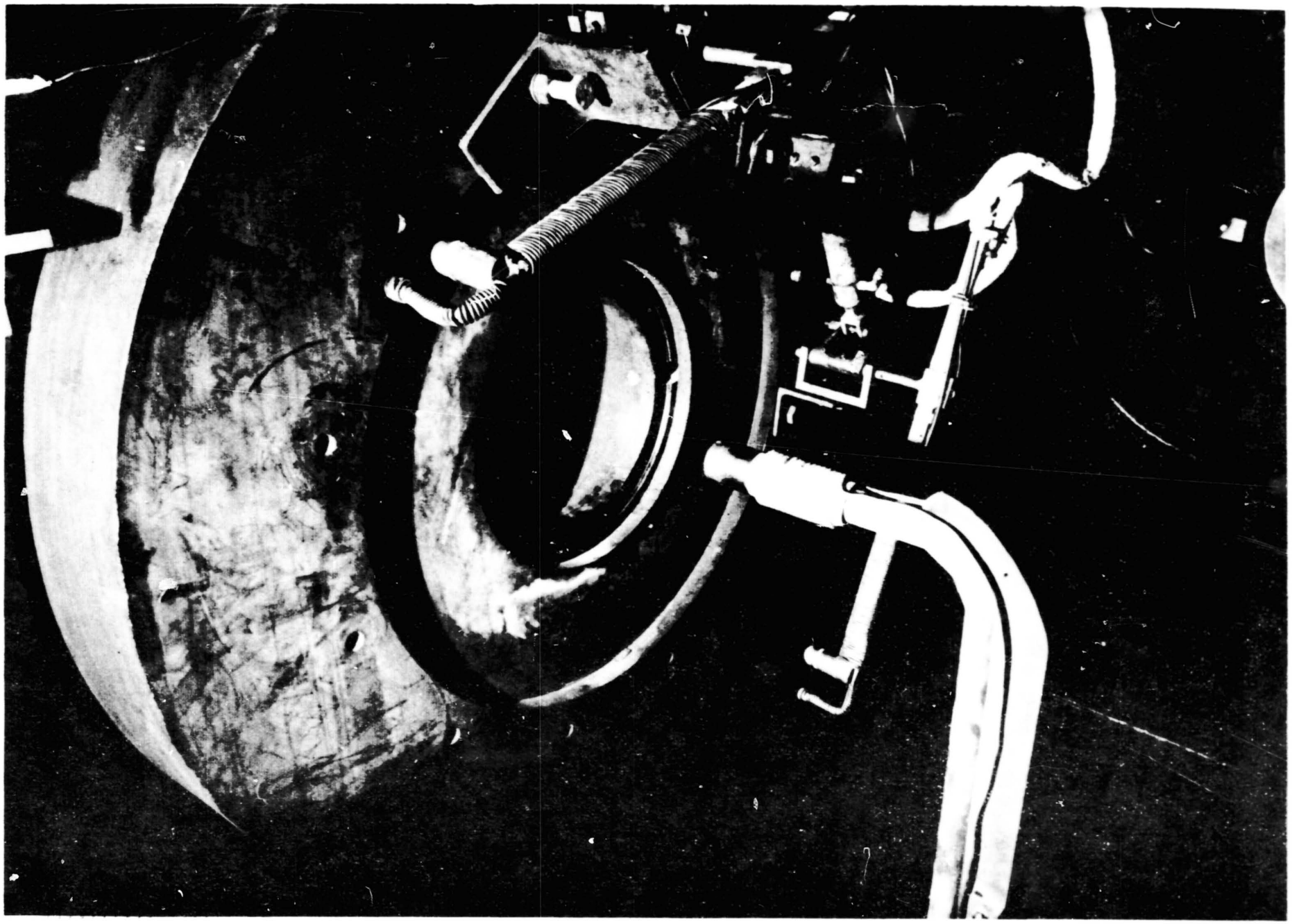

(a) Stagnation test.

Figure 3.- Sample supports mounted in test chamber.

NATIONAL AERONAUTICS AND SPACE ADMINISTRATION
AMES RESEARCH CENTER, MOFFETT FIELD, CALIFORNIA

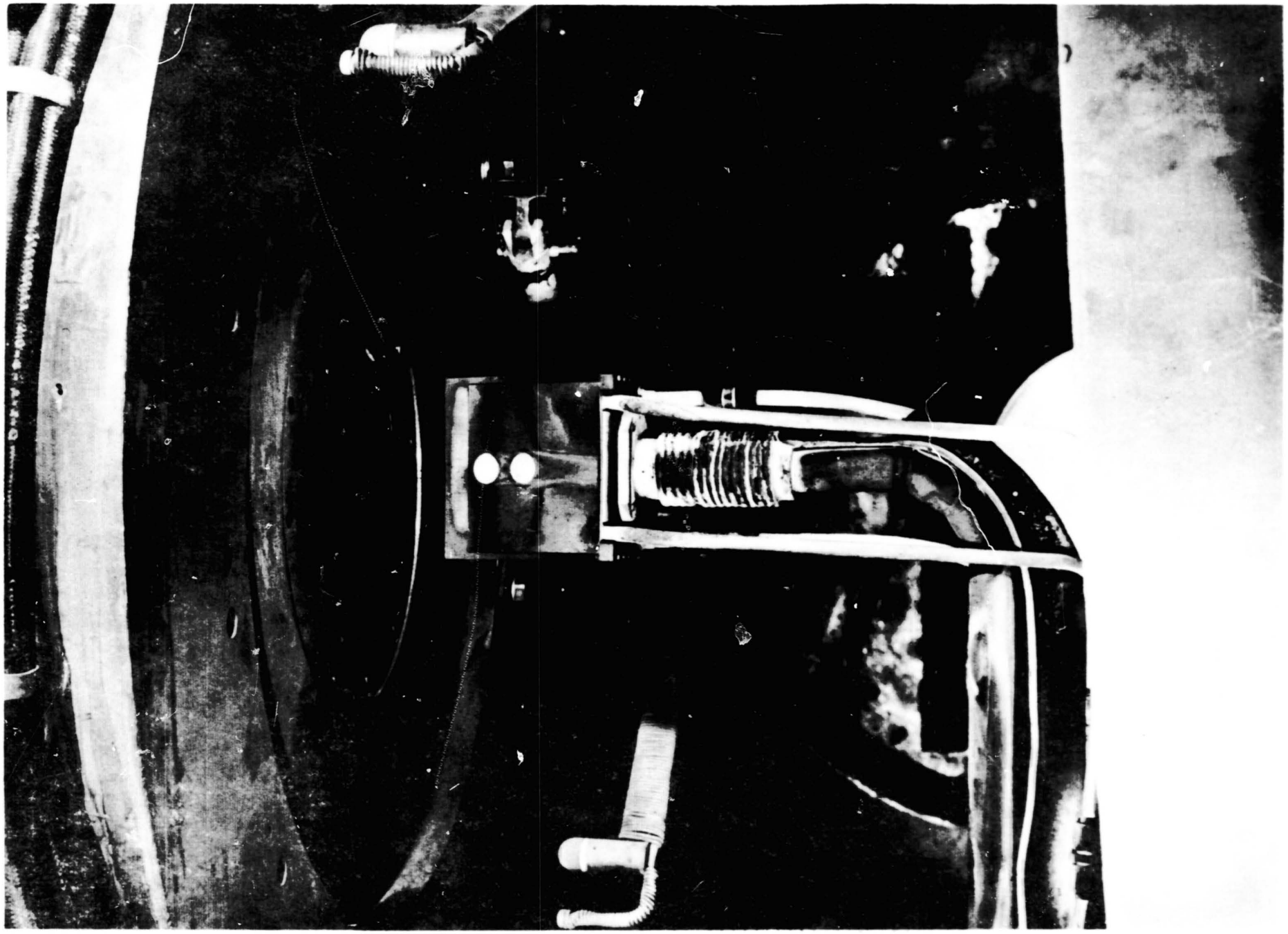

(b) Wedge test.

Figure 3.- Concluded.

NATIONAL AERONAUTICS AND SPACE ADMINISTRATION
AMES RESEARCH CENTER, MOFFETT FIELD, CALIFORNIA

National Aeronautics and Space Administration
Ames Research Center
Moffett Field, Calif.

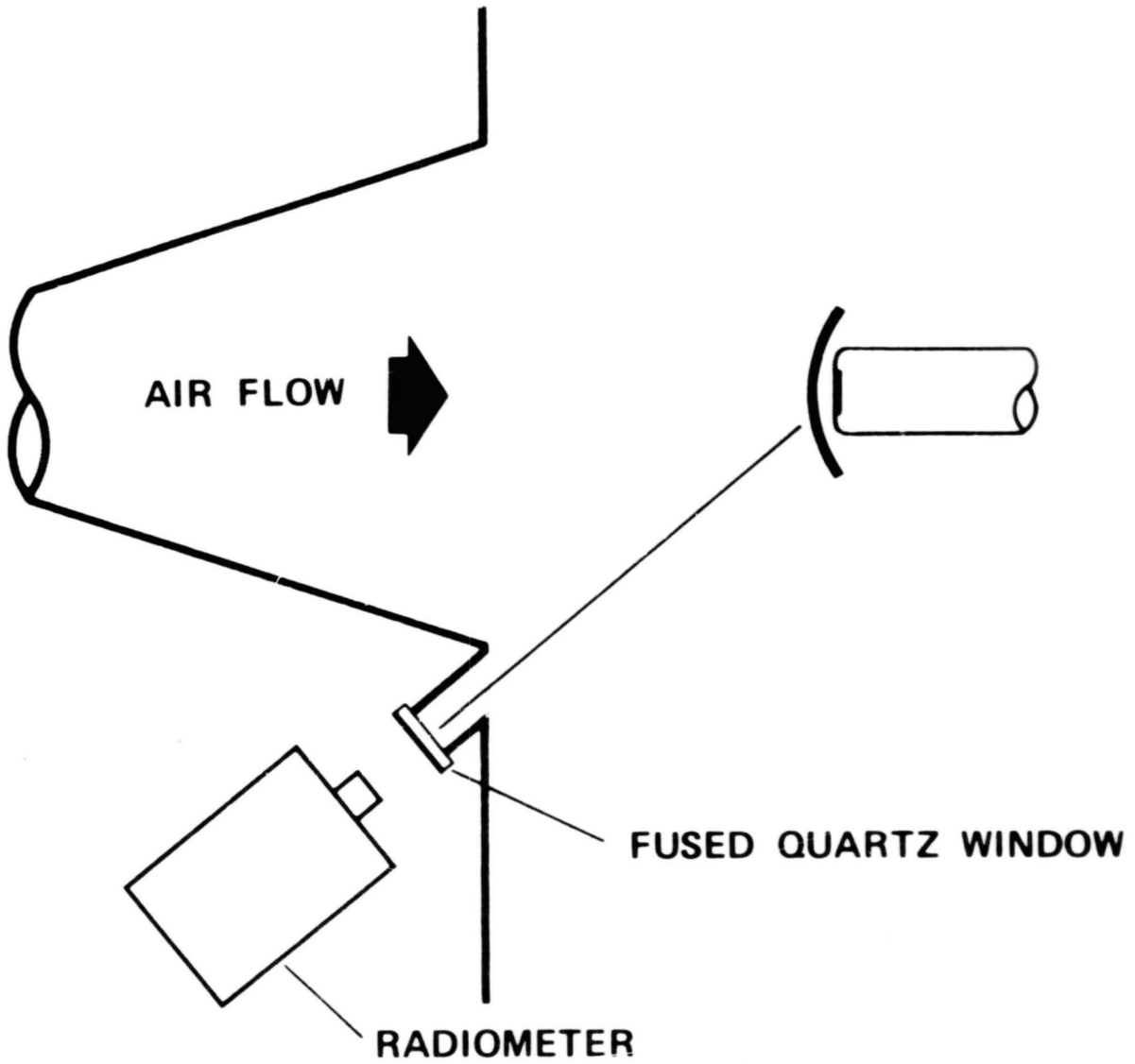

Figure 4.- Test arrangement for radiometric measurements.

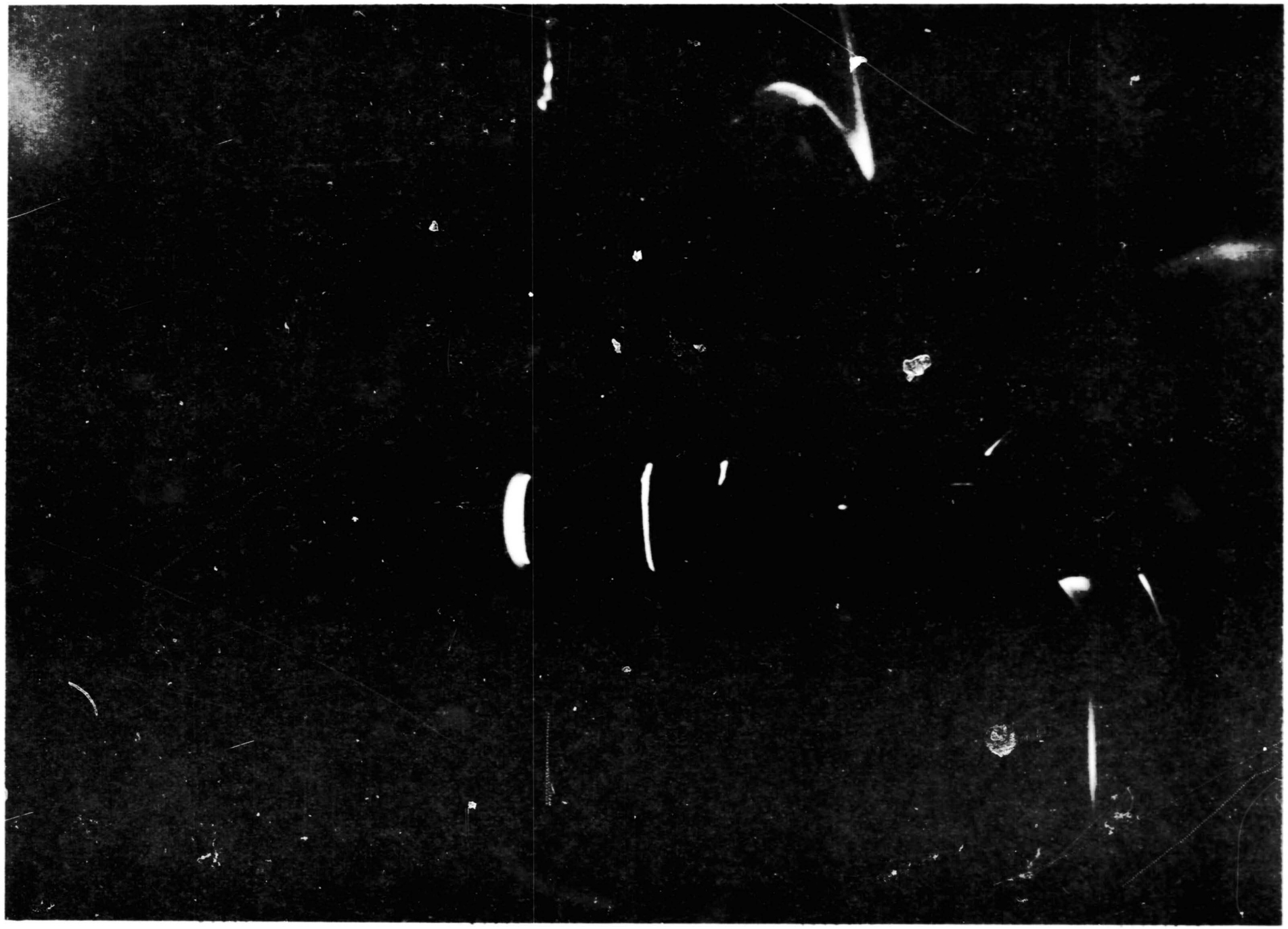

(a) Stagnation test.

Figure 5.- Photographs taken during typical test runs.

NATIONAL AERONAUTICS AND SPACE ADMINISTRATION
AMES RESEARCH CENTER MOFFETT FIELD CALIFORNIA

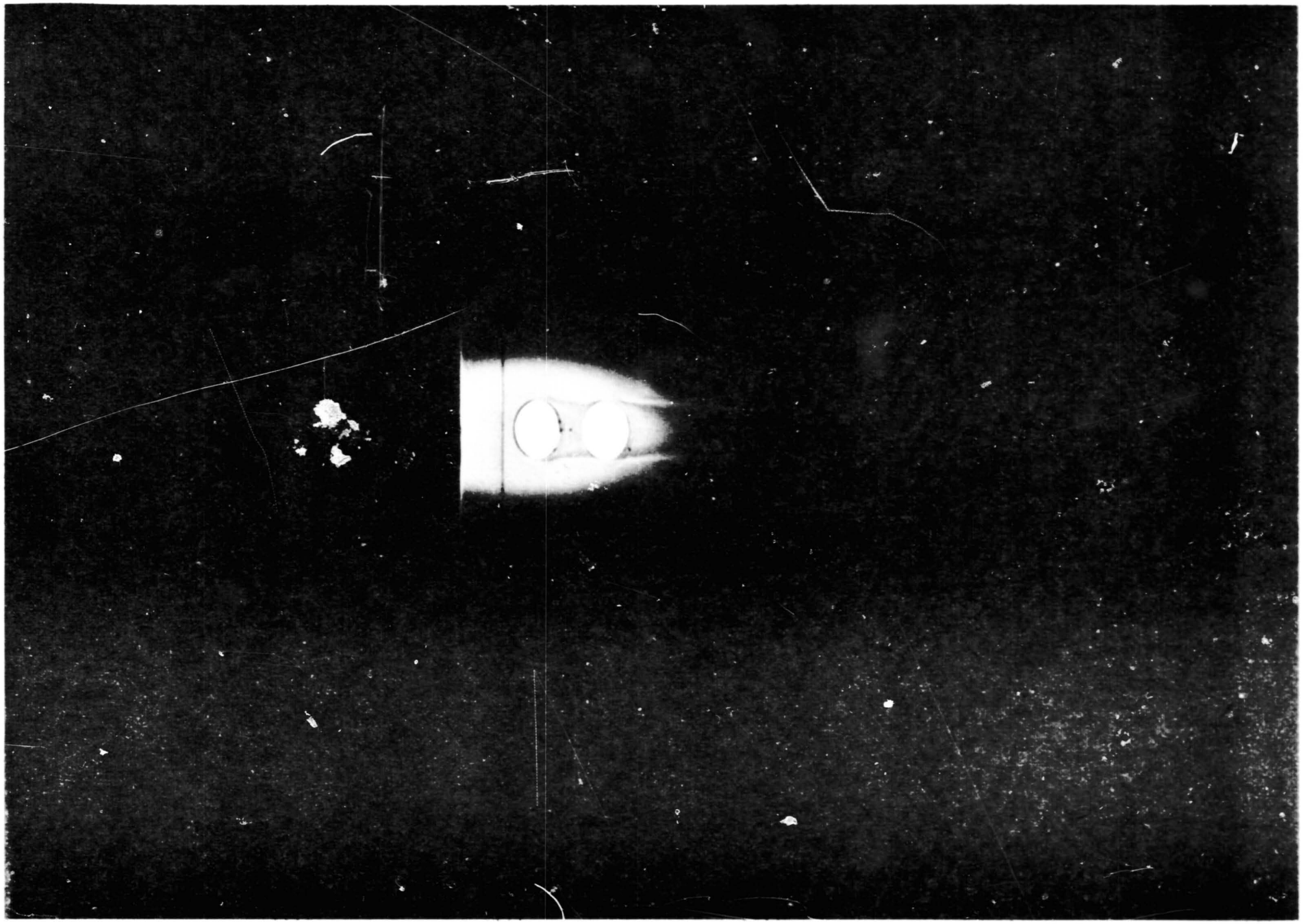

(b) Wedge test.

Figure 5.- Concluded.

NATIONAL AERONAUTICS AND SPACE ADMINISTRATION
AMES RESEARCH CENTER MOFFETT FIELD CALIFORNIA

A70-1878

(a) Stagnation test; TD-NiCr-2 after 12 cycles.

Figure 6.- Typical post run photographs.

NATIONAL AERONAUTICS AND SPACE ADMINISTRATION
AMES RESEARCH CENTER, MOFFETT FIELD, CALIFORNIA

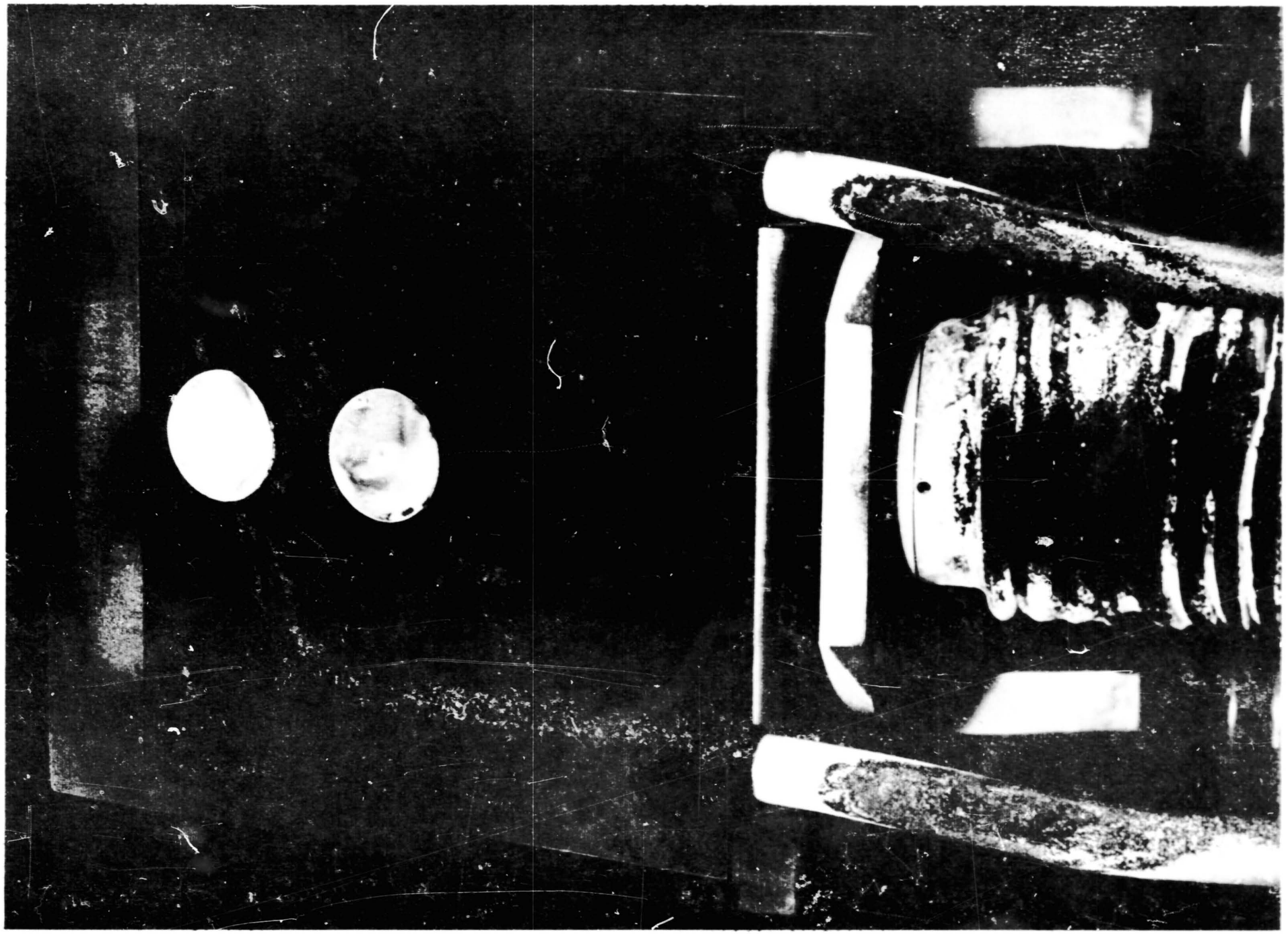

(b) Wedge test; after 28 cycles.

Figure 6.- Concluded.

NATIONAL AERONAUTICS AND SPACE ADMINISTRATION
AMES RESEARCH CENTER, MOFFETT FIELD, CALIFORNIA

A70-4126

(a) Stagnation test. TD-NiCr-1; T = 1800°F, P = 15 Torr, 50 cycles.

Figure 7.- Post test photographs of oxidized specimens.

NATIONAL AERONAUTICS AND SPACE ADMINISTRATION
AMES RESEARCH CENTER, MOFFETT FIELD, CALIFORNIA

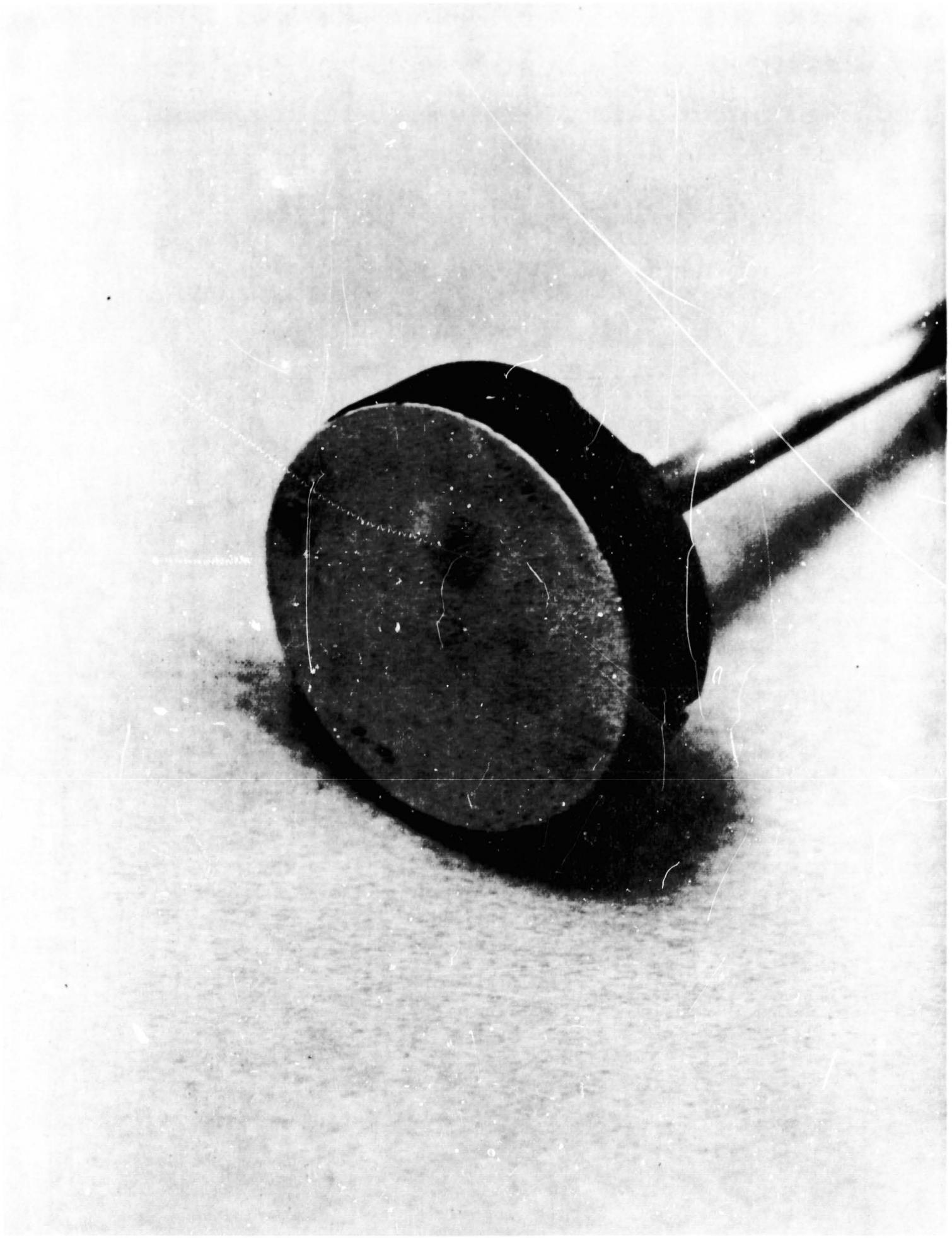

(b) Stagnation test. TD-NiCr-2; T = 2200°F, P = 15 Torr, 50 cycles.

Figure 7.- Continued.

NATIONAL AERONAUTICS AND SPACE ADMINISTRATION
AMES RESEARCH CENTER, MOFFETT FIELD, CALIFORNIA

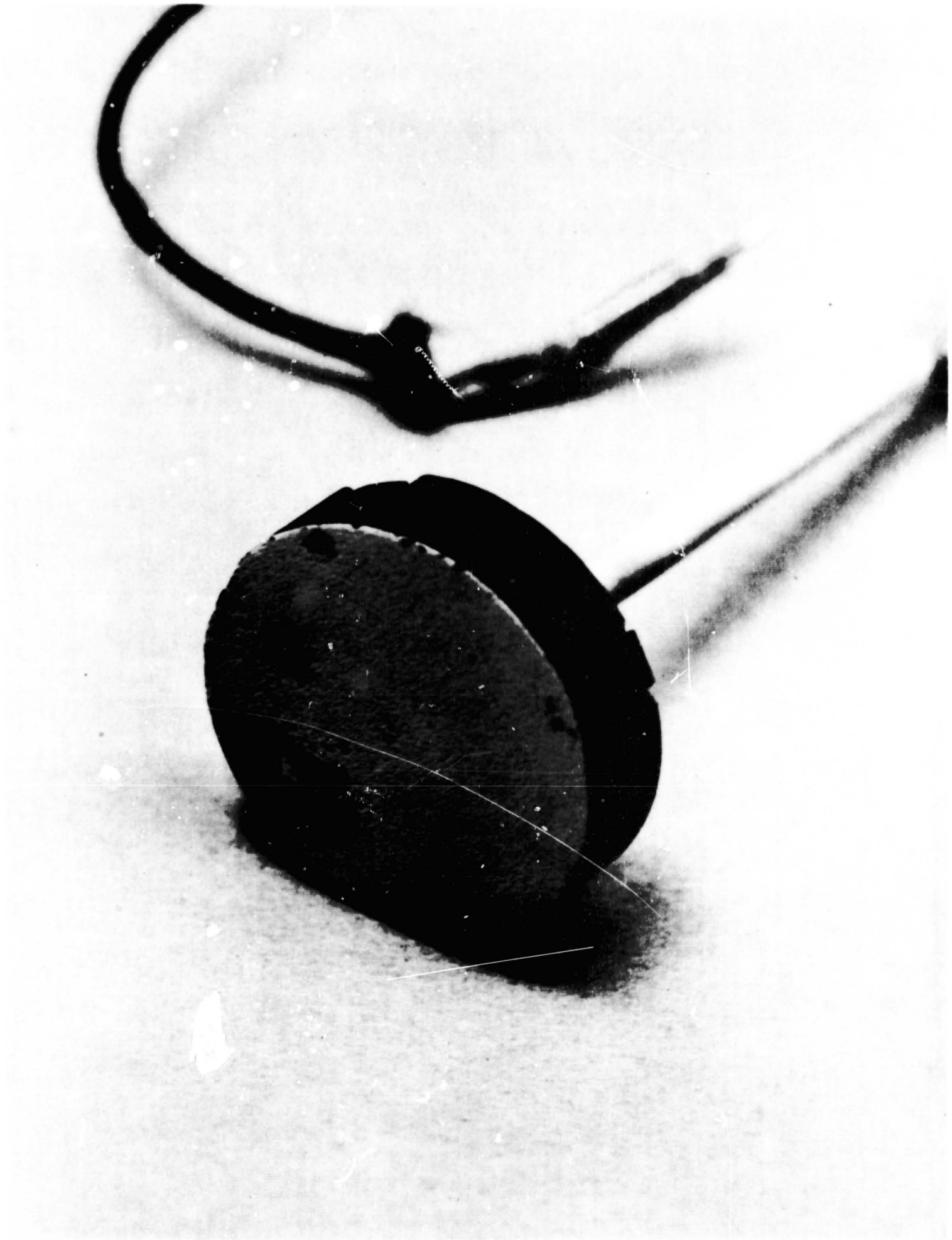

A70-4127

(c) Stagnation test. TD-NiCr-8; T = 2200°F, P = 30 Torr, 34 cycles.

Figure 7.- Continued.

NATIONAL AERONAUTICS AND SPACE ADMINISTRATION
AMES RESEARCH CENTER, MOFFETT FIELD, CALIFORNIA

A70-3298

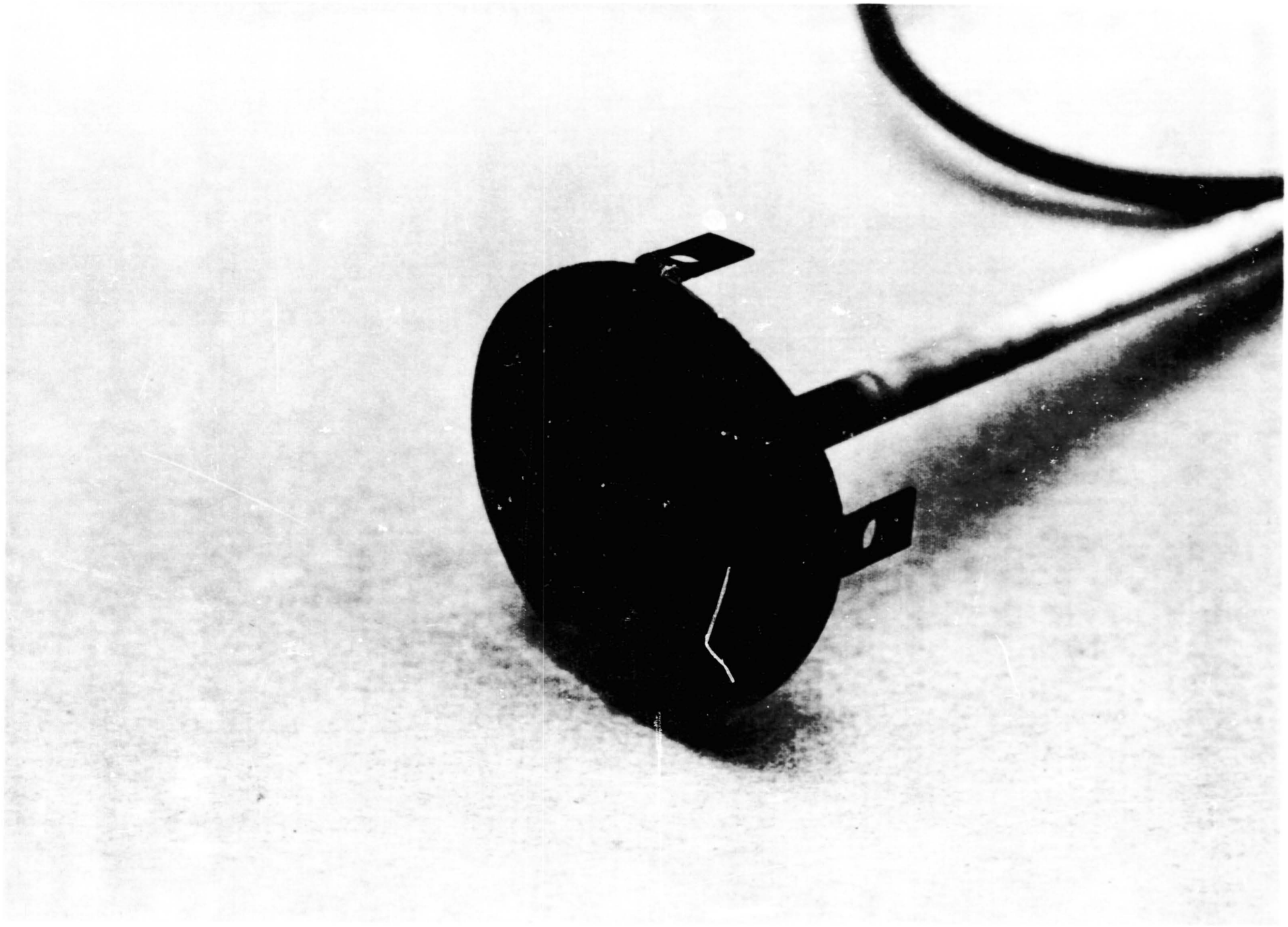

(d) Stagnation test. TD-NiCrAlY-2; T = 2200°F, P = 15 Torr, 40 cycles.

Figure 7.- Continued.

NATIONAL AERONAUTICS AND SPACE ADMINISTRATION
AMES RESEARCH CENTER, MOFFETT FIELD, CALIFORNIA

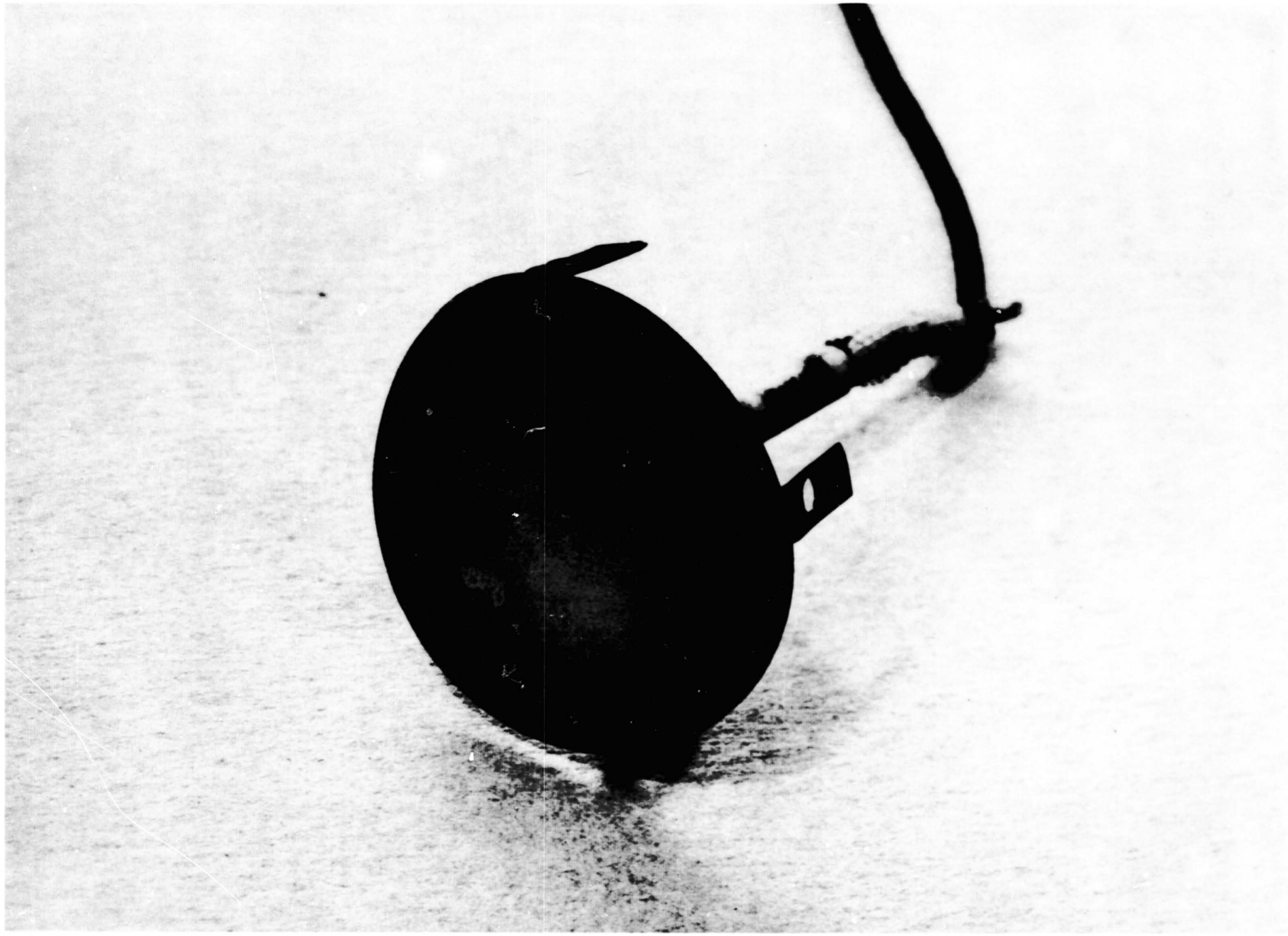

(e) Wedge test. TD-NiCr-6; T = 2200°F, P = 15 Torr, 28 cycles.

Figure 7.- Continued.

NATIONAL AERONAUTICS AND SPACE ADMINISTRATION
AMES RESEARCH CENTER, MOFFETT FIELD, CALIFORNIA

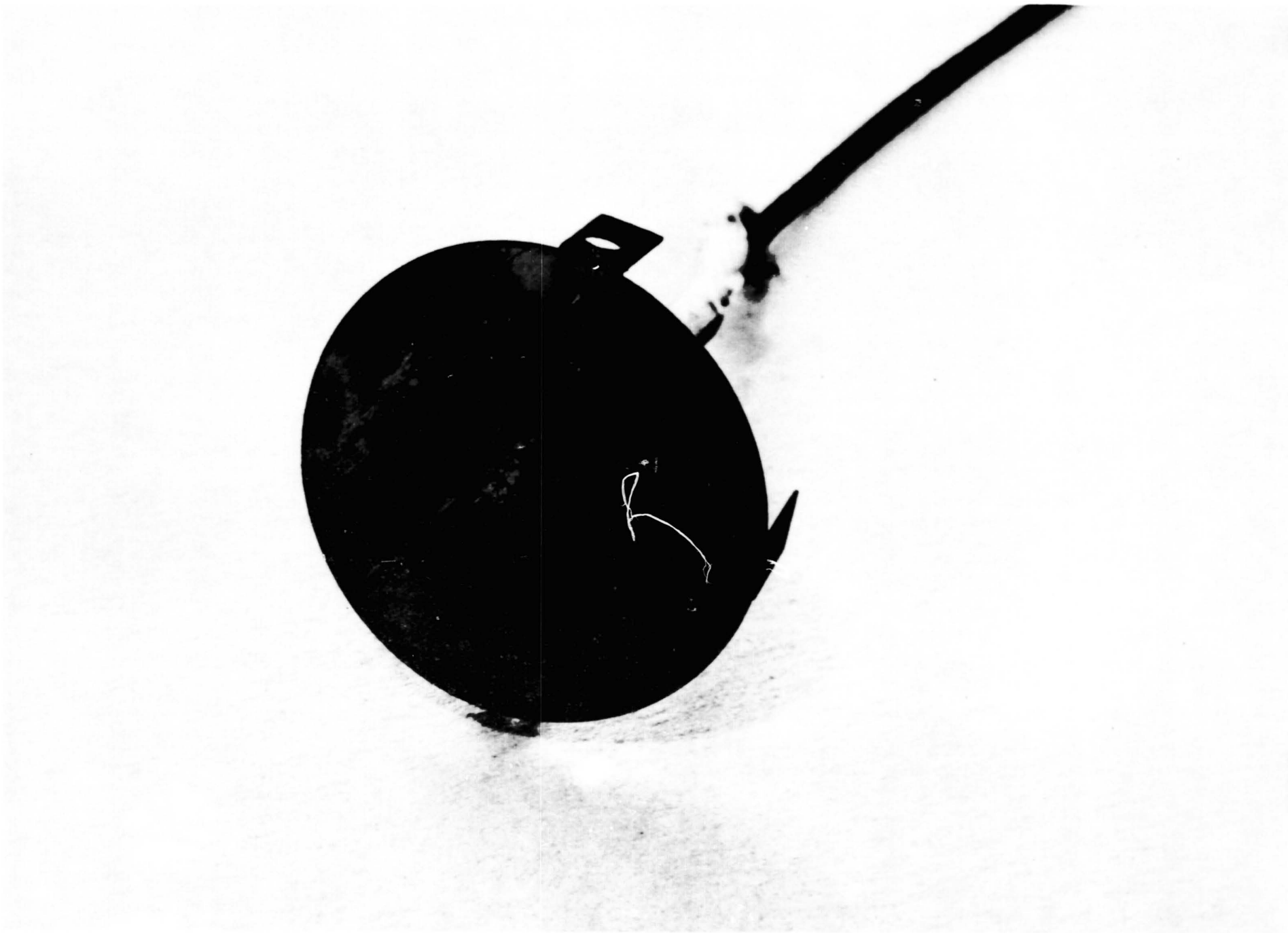

(f) Wedge test. TD-NiCr-7; T = 2000°F, P = 15 Torr, 28 cycles.

Figure 7.- Concluded.

National Aeronautics and Space Administration
Ames Research Center
Moffett Field, Calif.

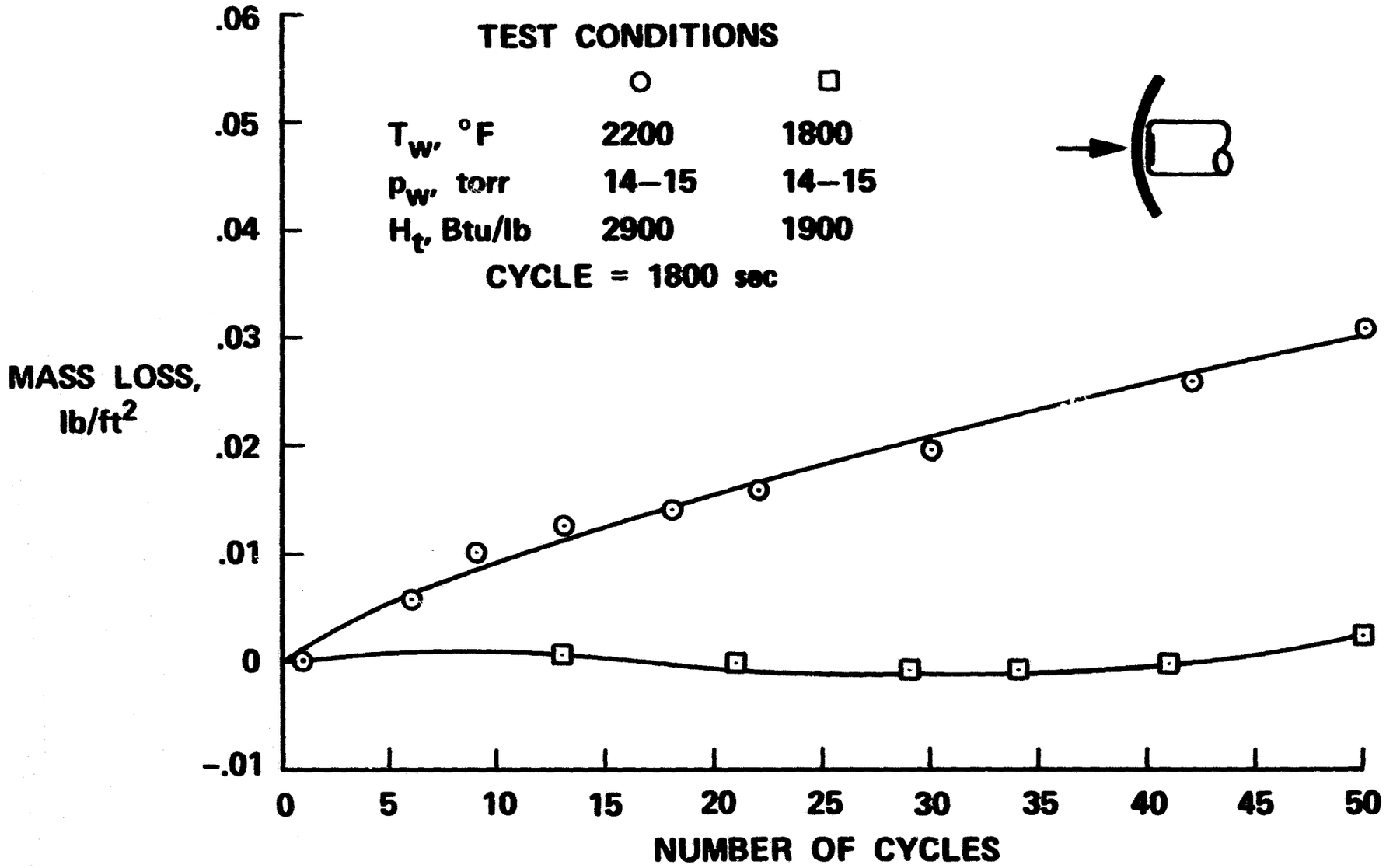

Figure 8.- The effect of temperature on the mass loss of TD-NiCr.

National Aeronautics and Space Administration
Ames Research Center
Moffett Field, Calif.

T_w = 2200°F CYCLE = 1800 sec

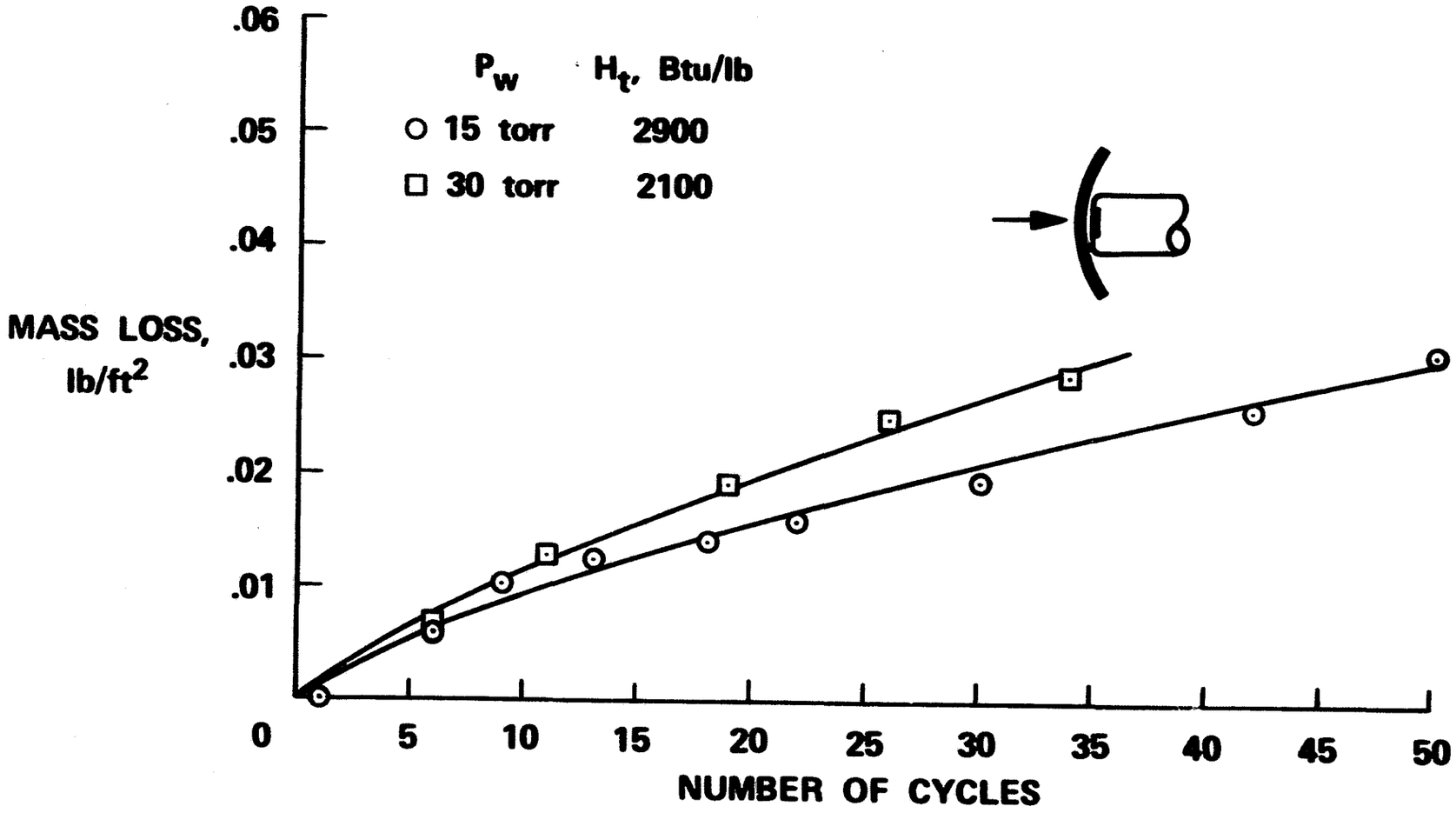

Figure 9.- The effect of pressure on the mass loss of TD-NiCr.

National Aeronautics and Space Administration
Ames Research Center
Moffett Field, Calif.

T_w = 2200°F p_w = 14-15 torr H_t = 2900 Btu/lb CYCLE = 1800 sec

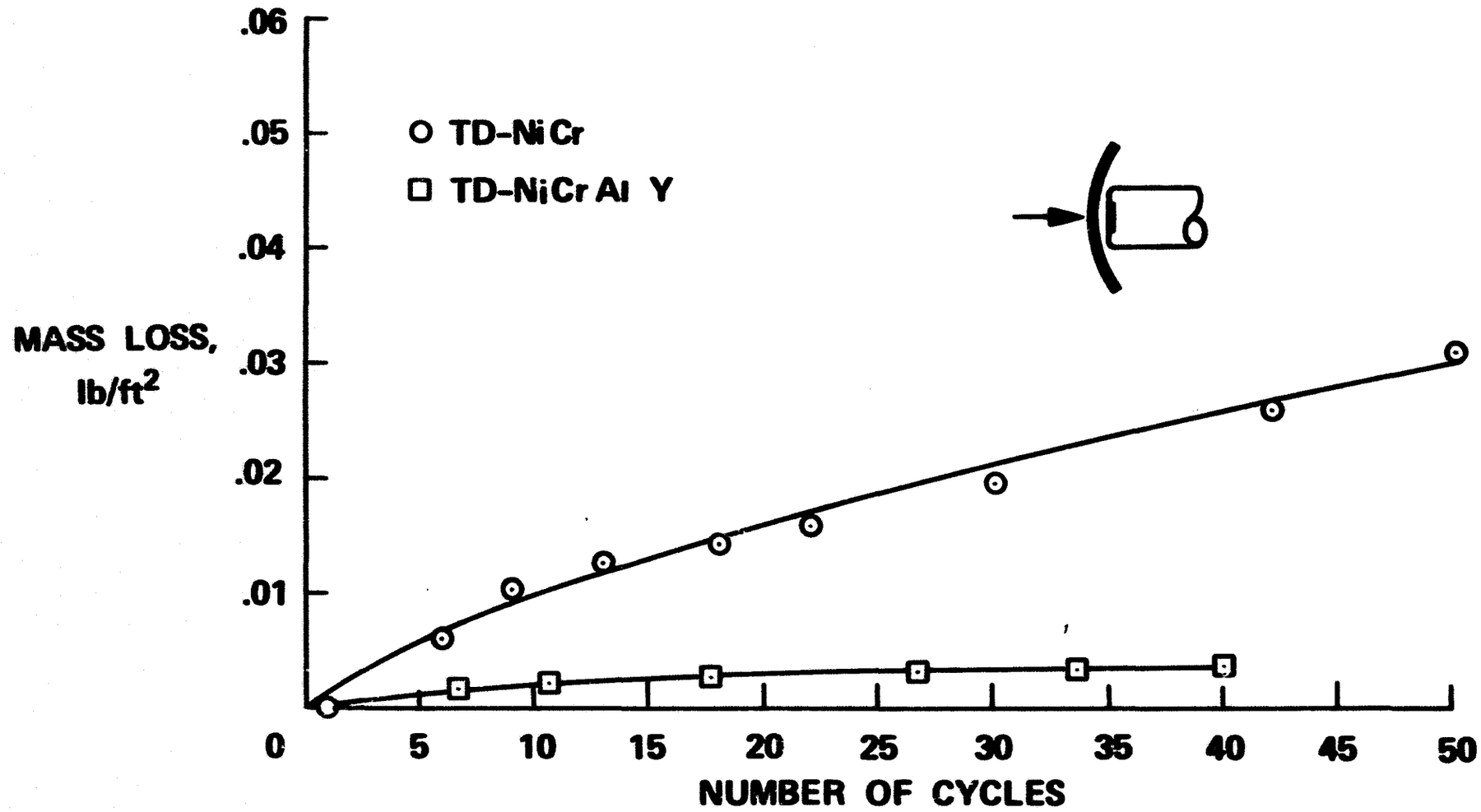

Figure 10.- Comparison of mass loss of TD-NiCr and TD-NiCrAlY.

National Aeronautics and Space Administration
Ames Research Center
Moffett Field, Calif.

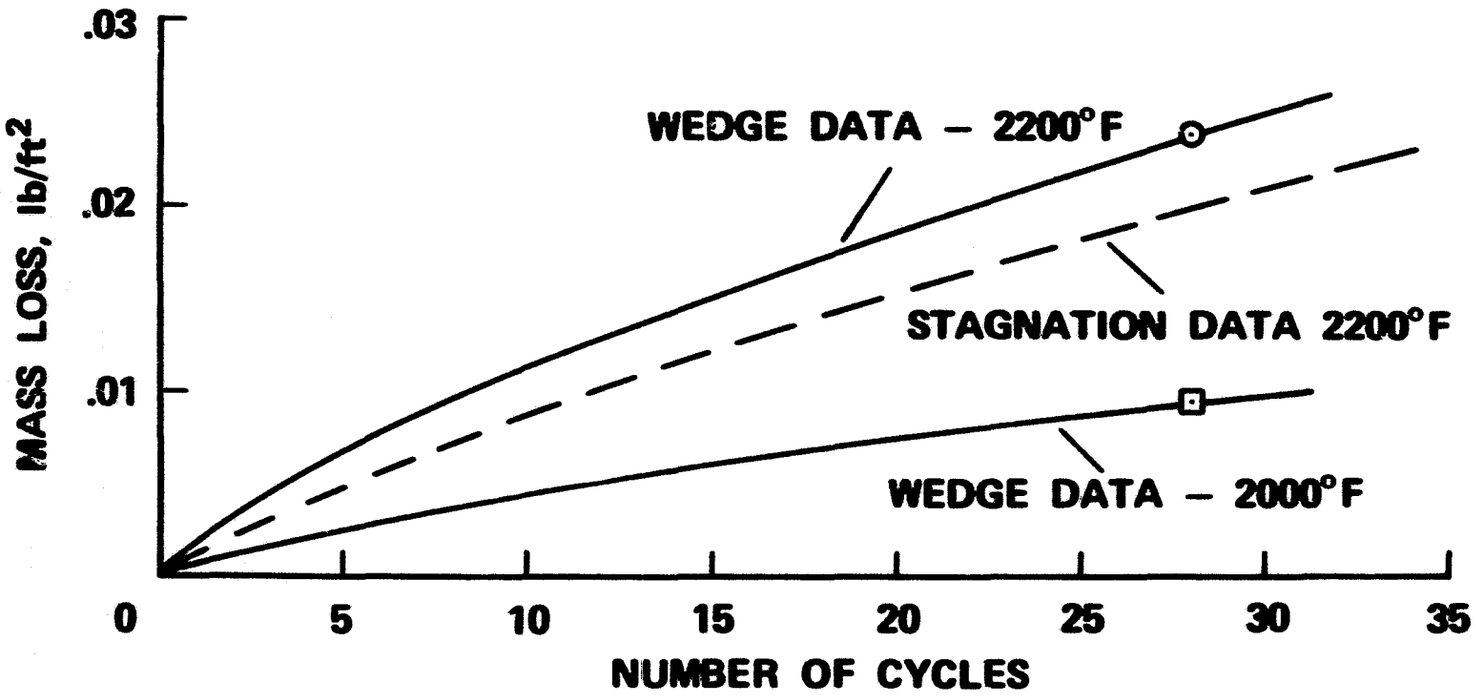

Figure 11.- Mass losses of wedge test compared with stagnation test.

National Aeronautics and Space Administration
Ames Research Center
Moffett Field, Calif.

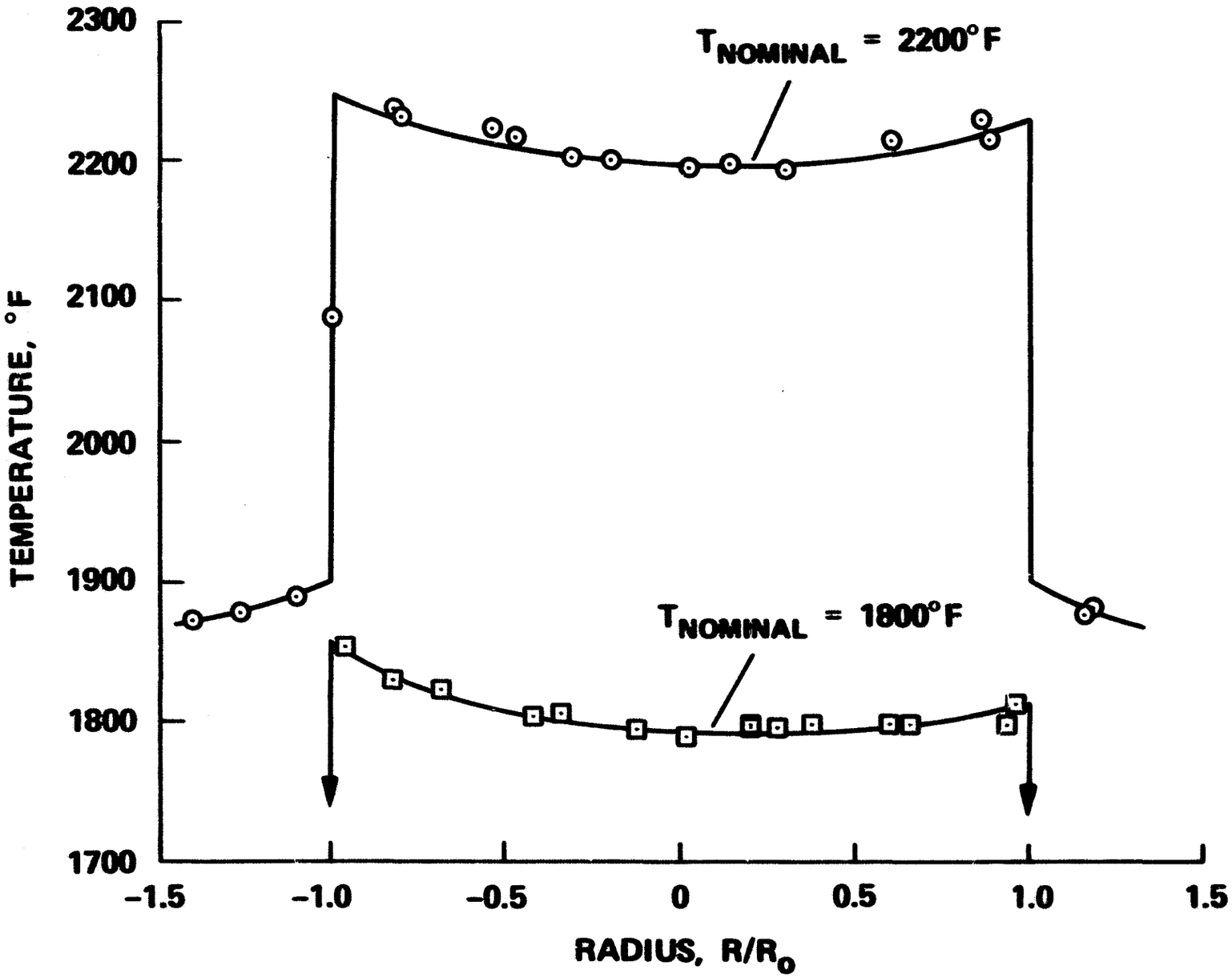

Figure 12.- Typical temperature distributions measured with radiometer.

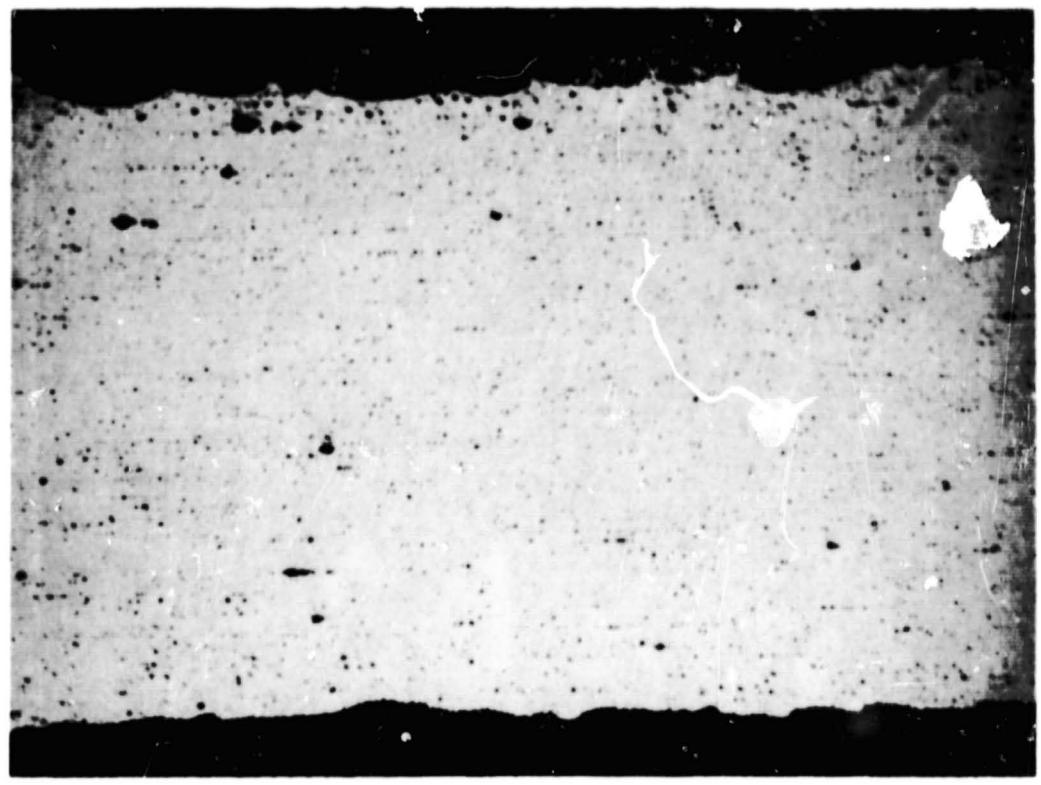

(a) UNETCHED. X250.

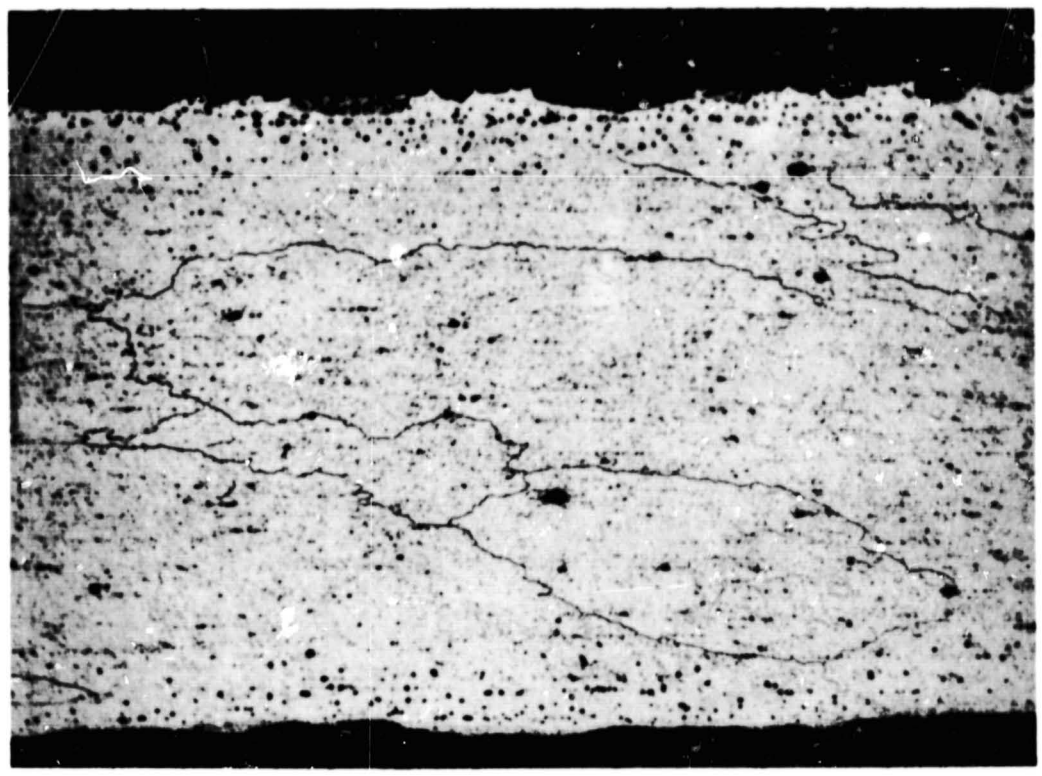

(b) ETCHED ELECTROLYTICALLY. X250

Figure 13.- Microstructure of TD-NiCr-1. Stagnation test. T = 1800°F, P = 15 Torr. Courtesy of Lewis Research Center.

NATIONAL AERONAUTICS AND SPACE ADMINISTRATION
AMES RESEARCH CENTER, MOFFETT FIELD, CALIFORNIA

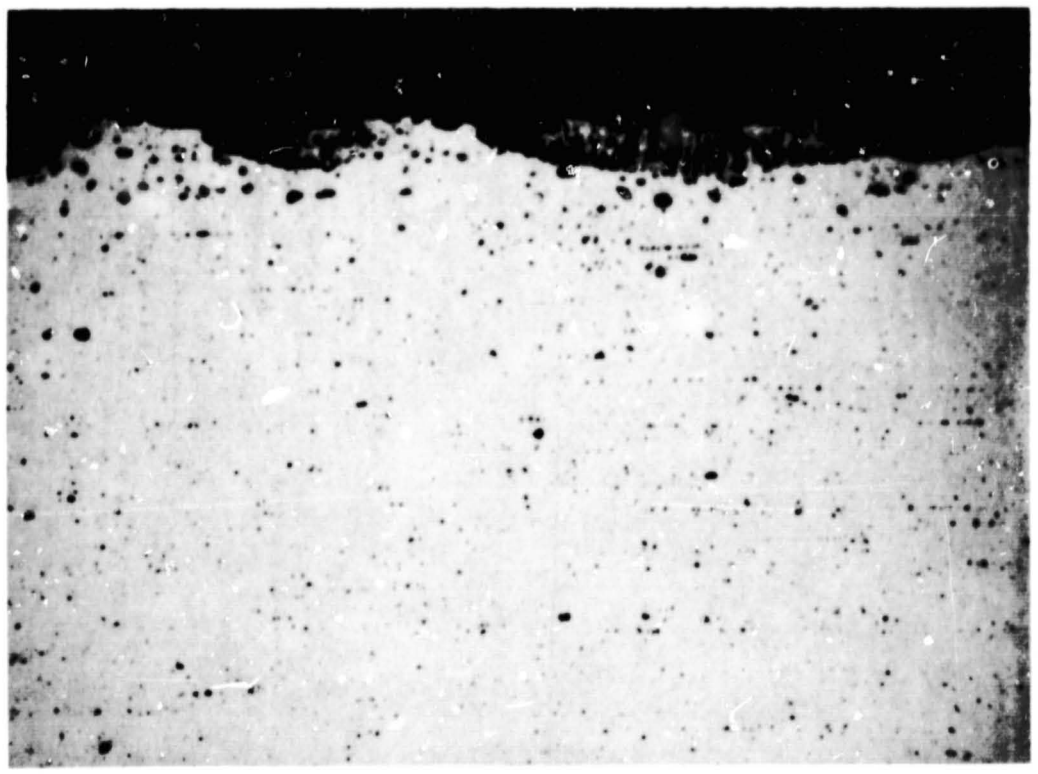

FRONT SIDE

(c) UNETCHED. X500

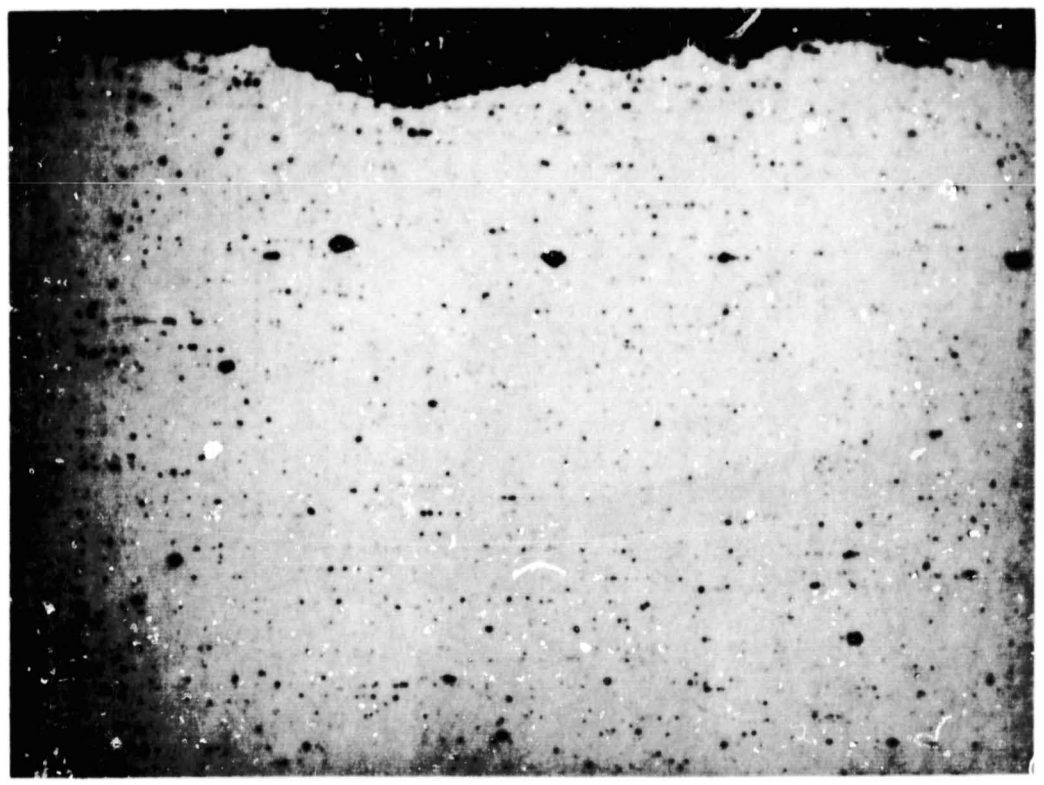

BACK SIDE

(d) UNETCHED. X500

Figure 13.- Concluded.

NATIONAL AERONAUTICS AND SPACE ADMINISTRATION
AMES RESEARCH CENTER, MOFFETT FIELD, CALIFORNIA

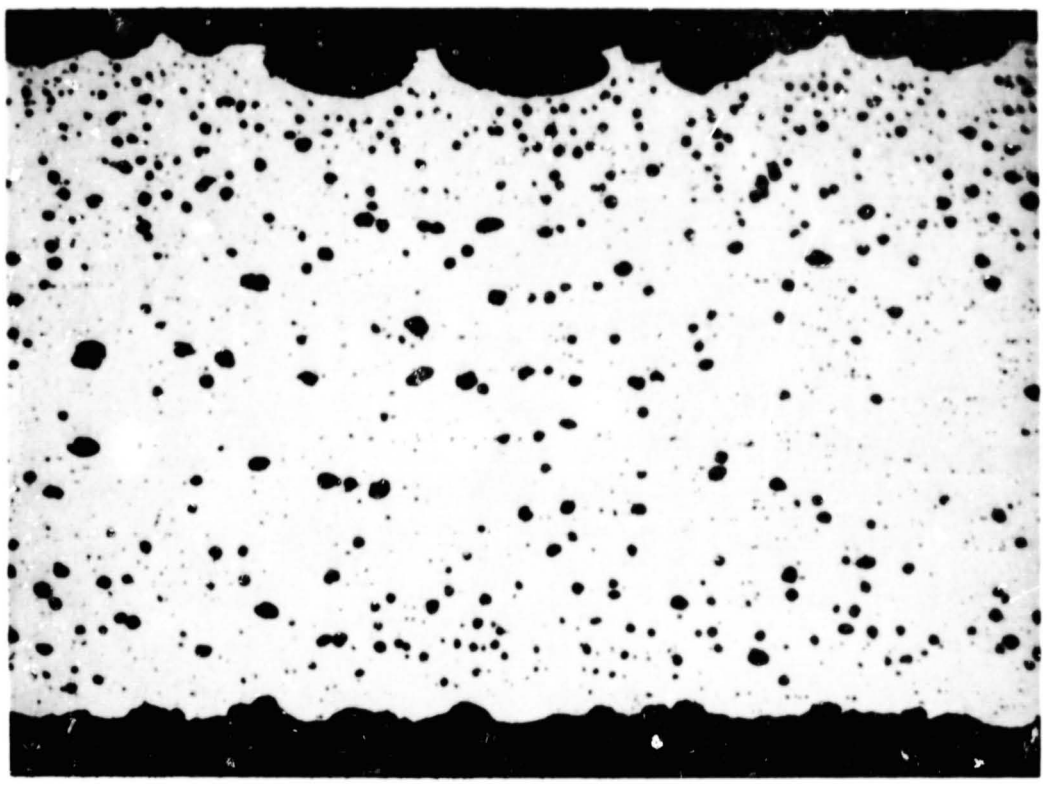

(a) UNETCHED. X250

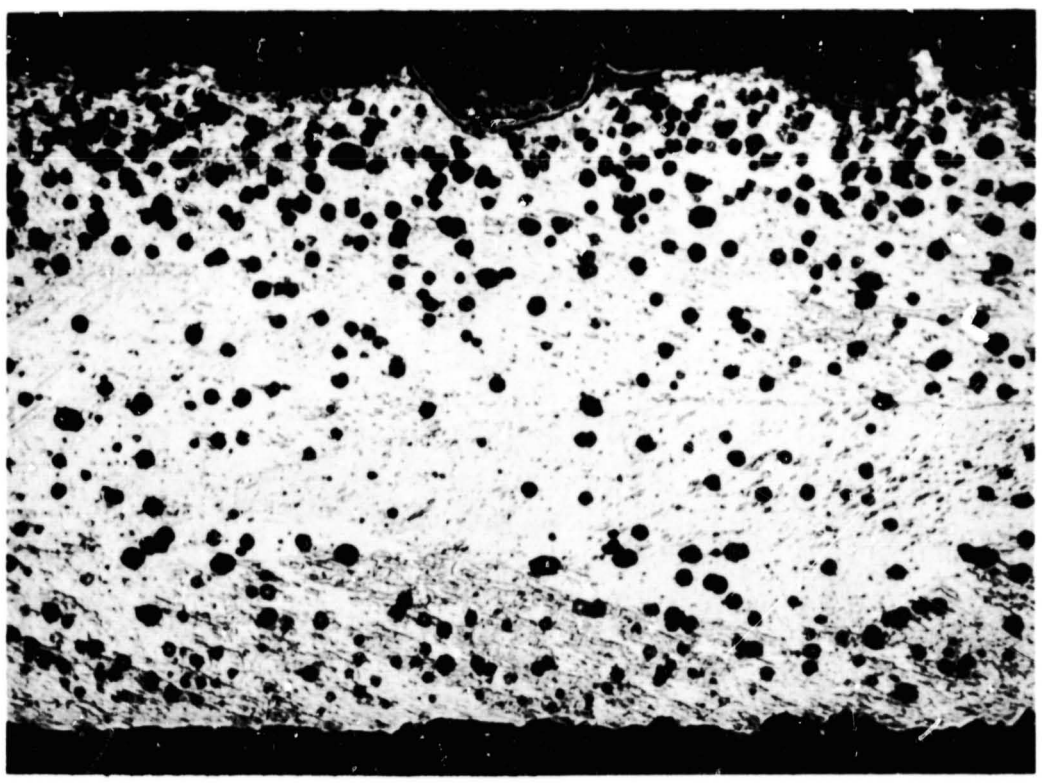

(b) ETCHED ELECTROLYTICALLY. X250

Figure 14.- Microstructure of TD-NiCr-2. Stagnation test. T = 2200°F, P = 15 Torr. Courtesy of Lewis Research Center.

NATIONAL AERONAUTICS AND SPACE ADMINISTRATION
AMES RESEARCH CENTER, MOFFETT FIELD, CALIFORNIA

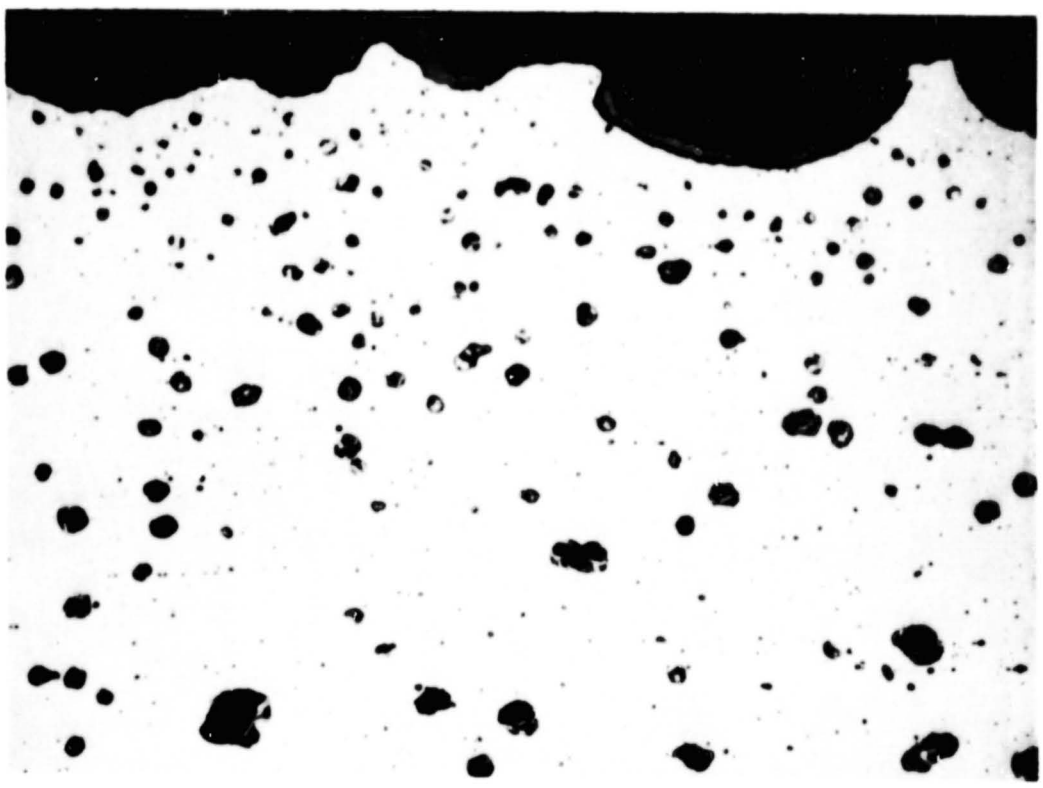

(c) UNETCHED. X500

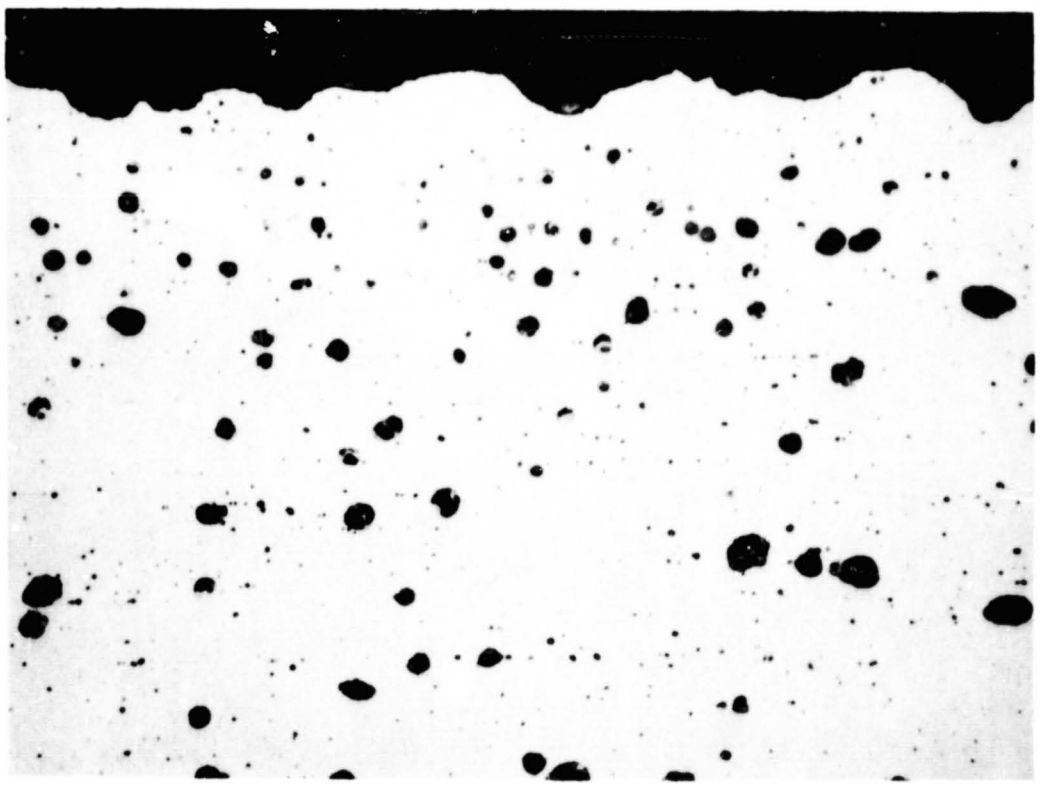

(d) UNETCHED. X500

Figure 14.- Concluded.

NATIONAL AERONAUTICS AND SPACE ADMINISTRATION
AMES RESEARCH CENTER, MOFFETT FIELD, CALIFORNIA

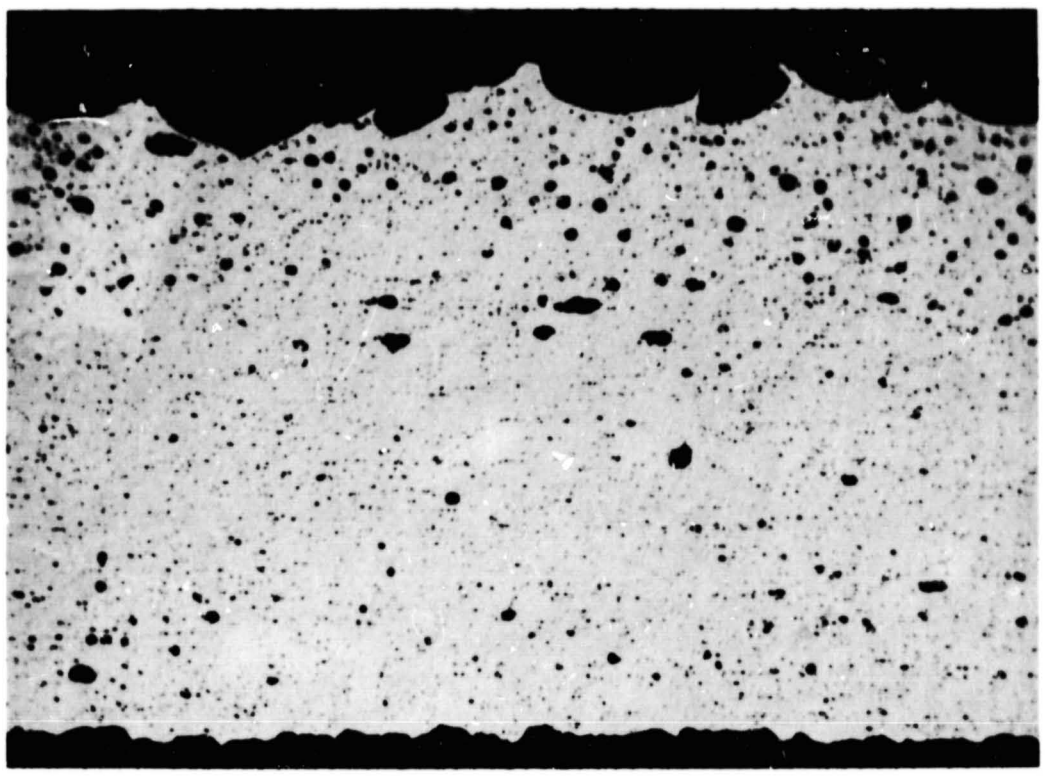

Figure 15.- Microstructure of TD-NiCr-8. Unetched. X250. Stagnation test. T = 2200°F, P = 15 Torr. Courtesy of Lewis Research Center.

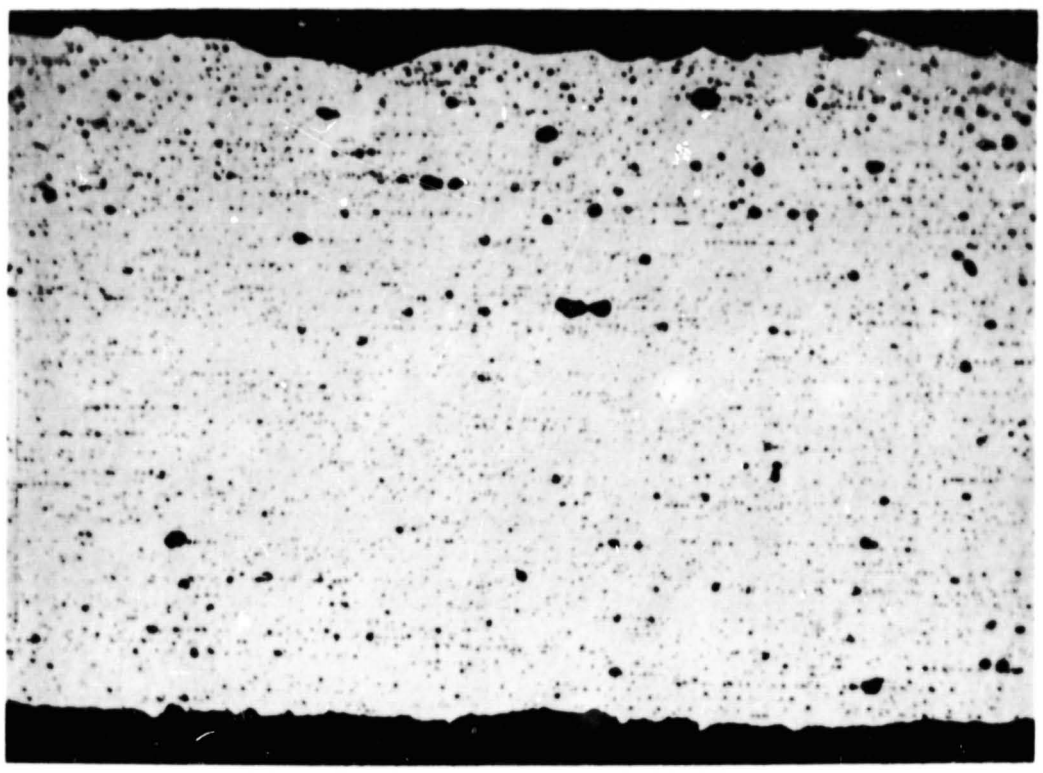

(a) TD-NiCr-6. T = 2200° F.

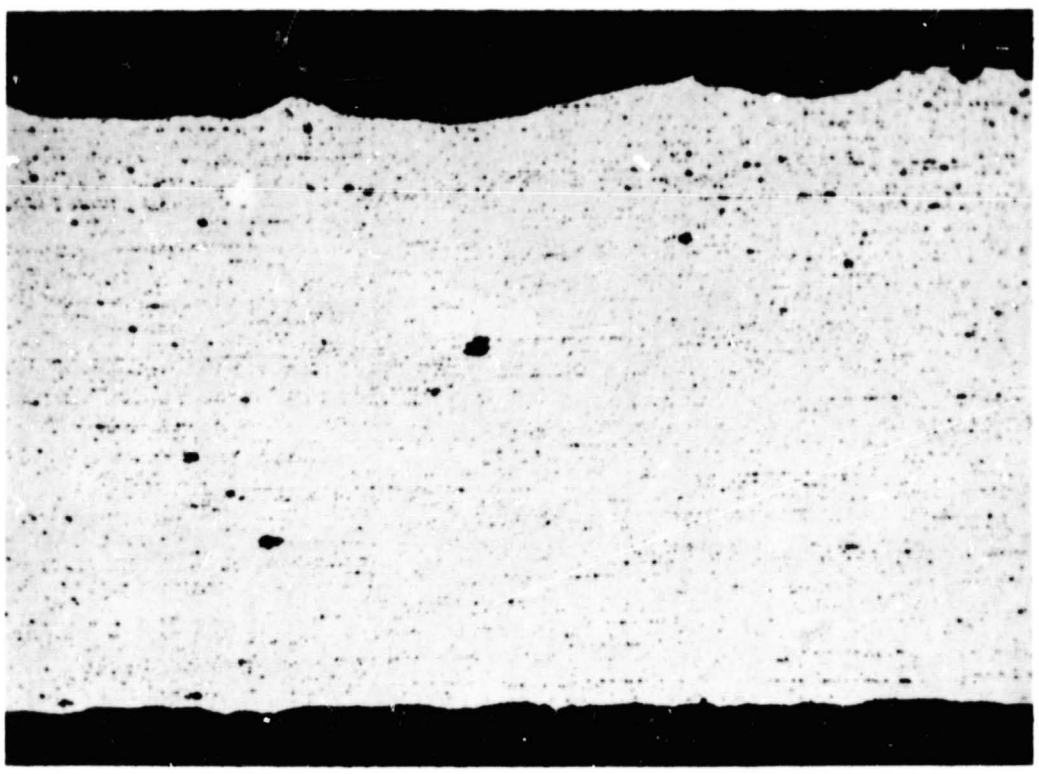

(b) TD-NiCr-7. T=2000° F.

Figure 16.- Microstructure of TD-NiCr-6 and TD-NiCr-7. Unetched. X250. Wedge test. P = 15 Torr. Courtesy of Lewis Research Center.

NATIONAL AERONAUTICS AND SPACE ADMINISTRATION
AMES RESEARCH CENTER, MOFFETT FIELD, CALIFORNIA

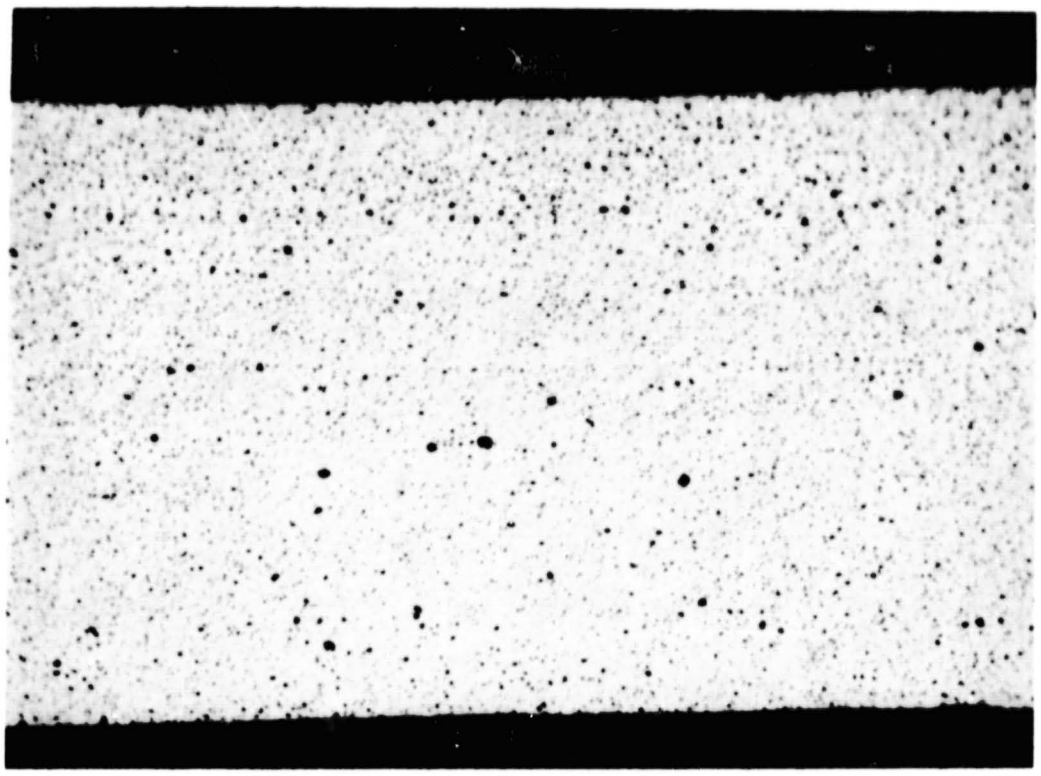

(a) AS RECEIVED, BEFORE ARC-JET EXPOSURE

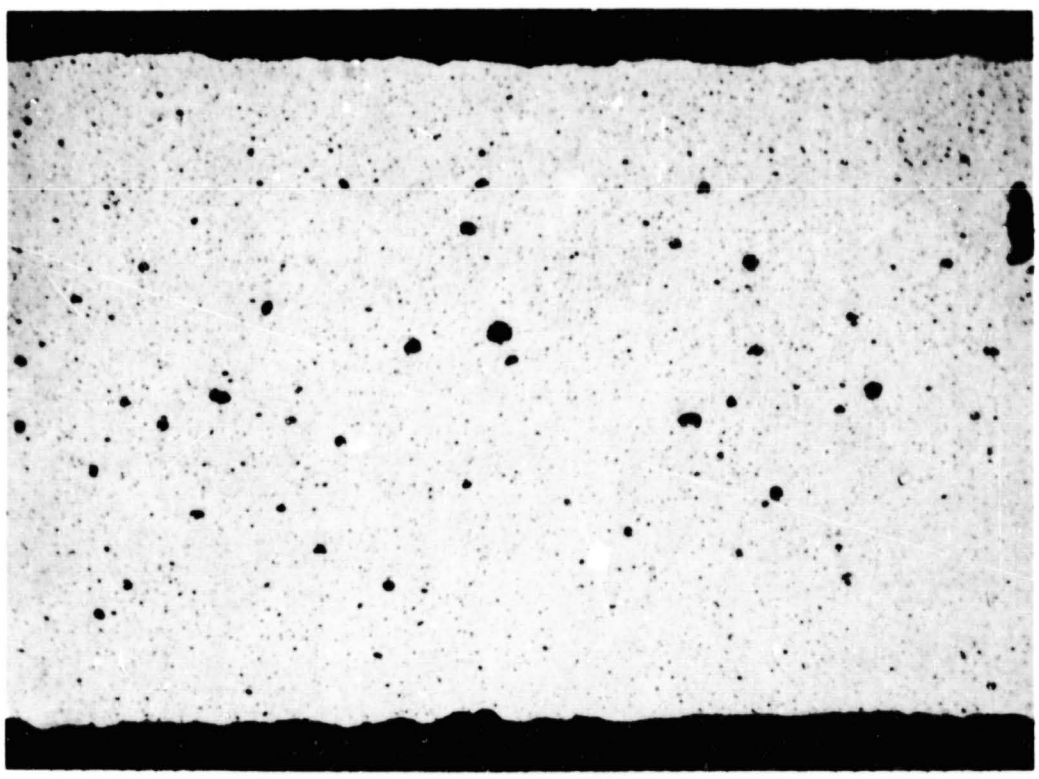

(b) AFTER ARC-JET EXPOSURE

Figure 17.- Microstructure of TD-NiCrAlY-2. Unetched. X250. Stagnation test. T = 2200°F, P = 15 Torr. Courtesy of Lewis Research Center.

National Aeronautics and Space Administration
Ames Research Center
Moffett Field, Calif.

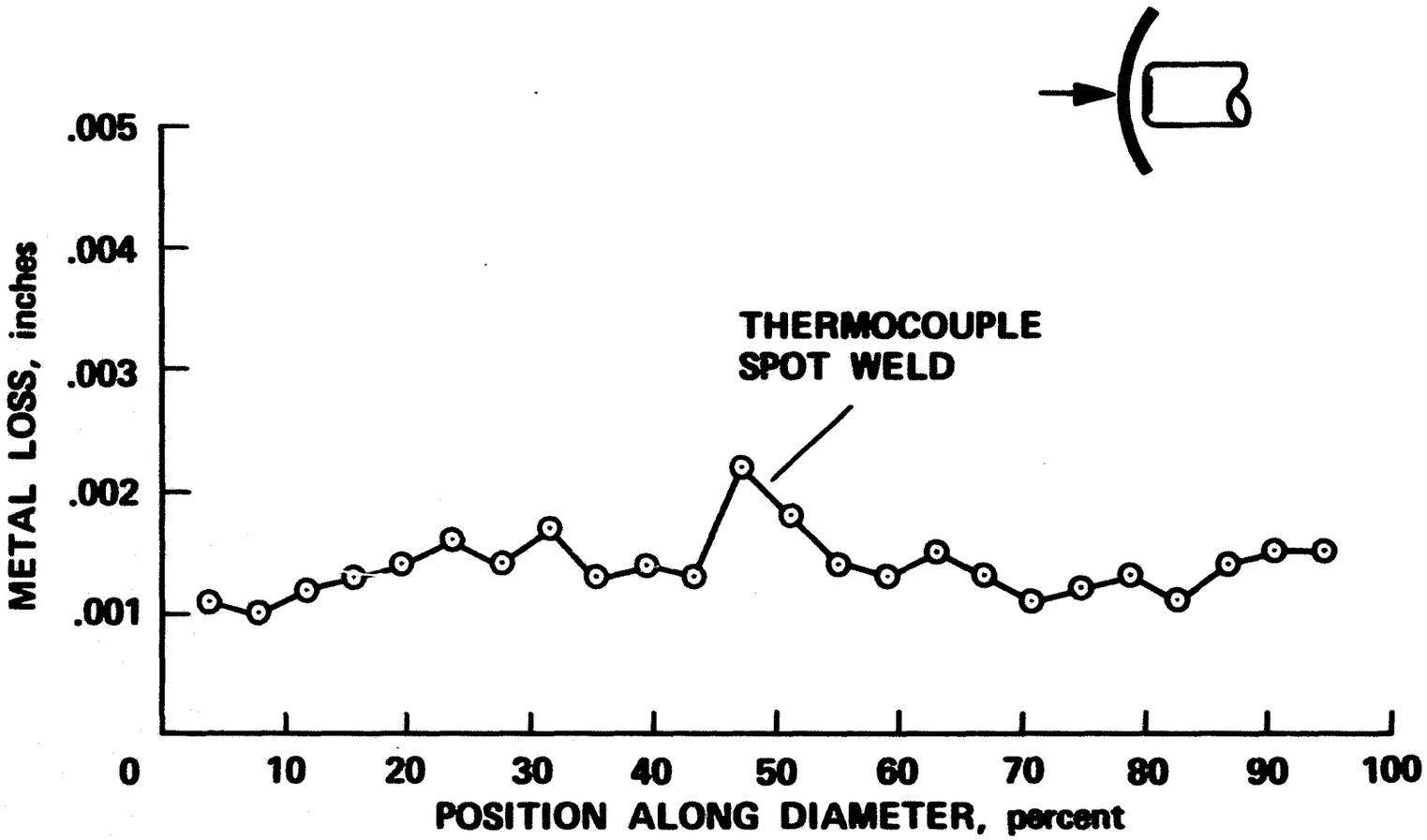

(a) TD-NiCr-1; T = 1800°F, P = 15 Torr.

Figure 18.- Metal loss along cross section of specimens. Courtesy of Lewis Research Center.

National Aeronautics and Space Administration
Ames Research Center
Moffett Field, Calif.

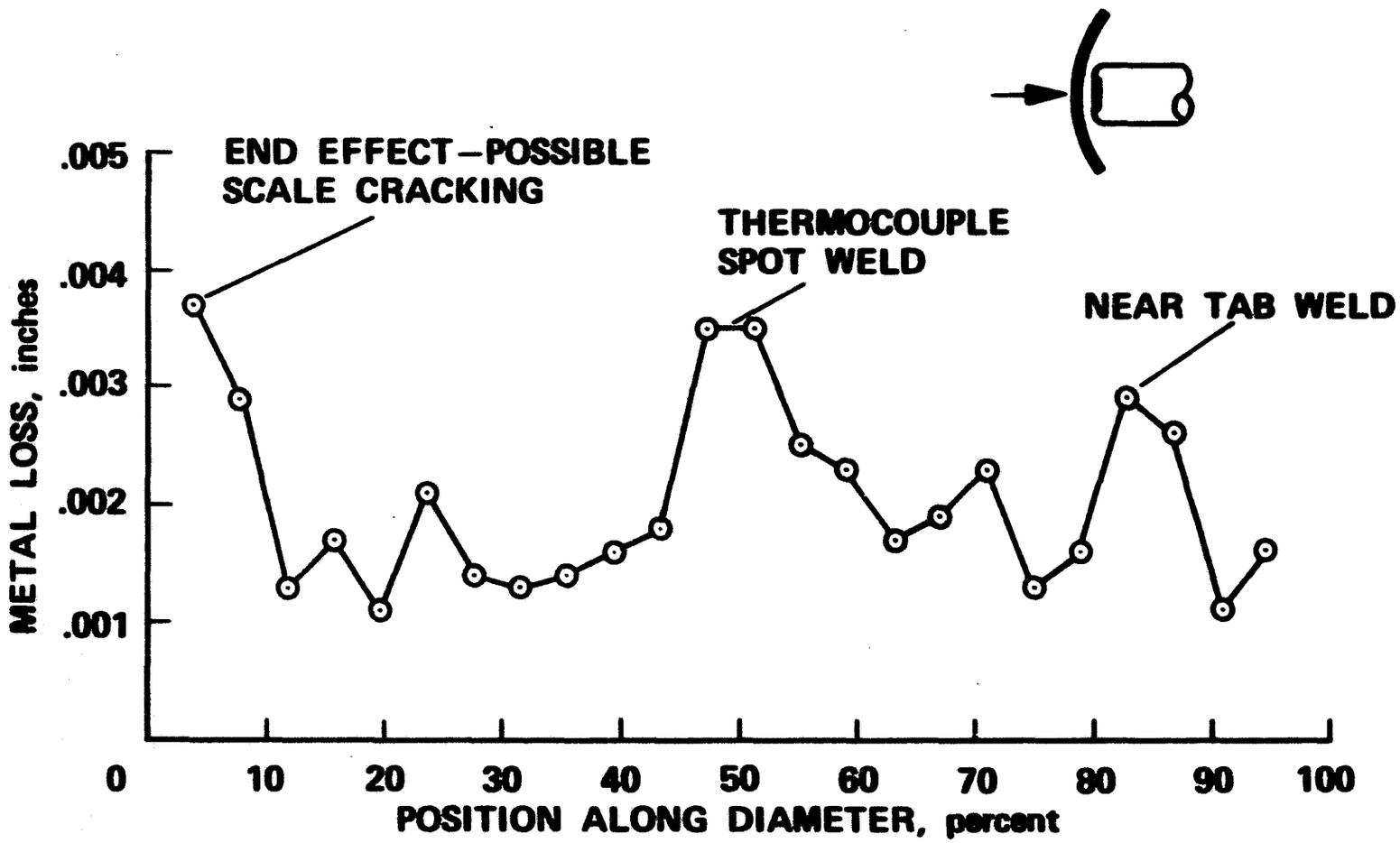

(b) TD-NiCr-2; T = 2200°F, P = 15 Torr.

Figure 18.- Continued.

National Aeronautics and Space Administration
Ames Research Center
Moffett Field, Calif.

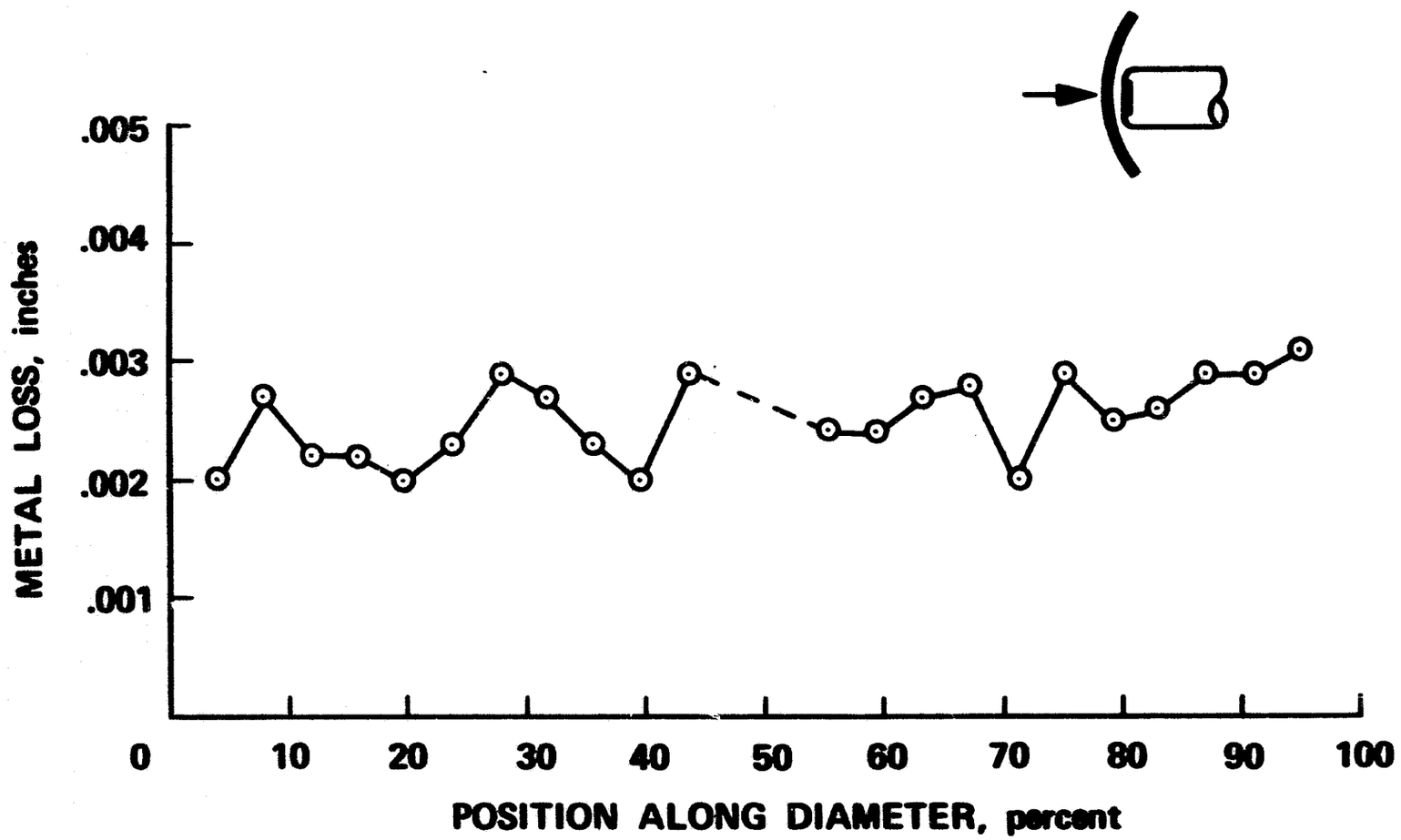

(c) TD-NiCr-8; T = 2200°F, P = 30 Torr.

Figure 18.- Continued.

National Aeronautics and Space Administration
Ames Research Center
Moffett Field, Calif.

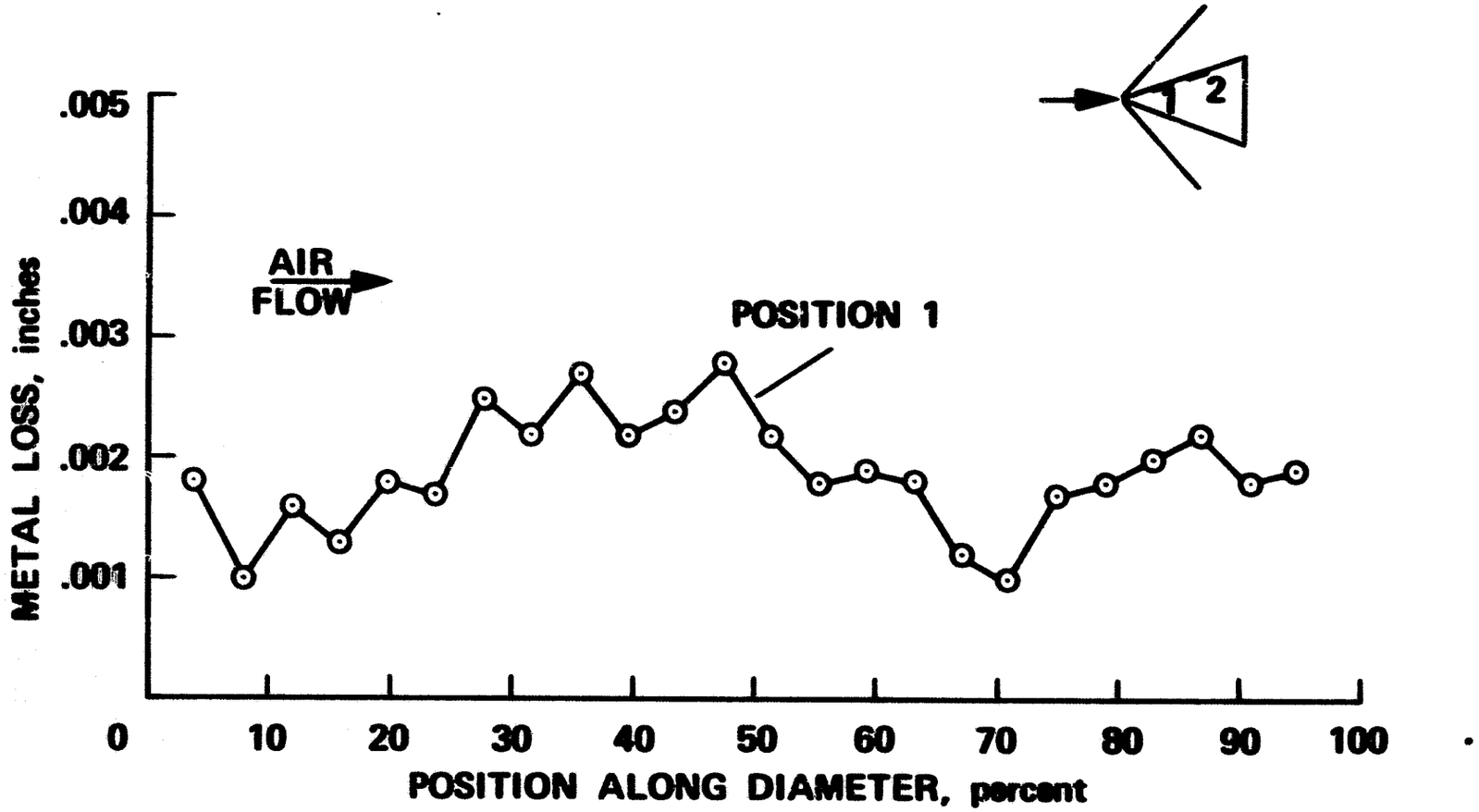

(d) TD-NiCr-6; T = 2200°F, P = 15 Torr.

Figure 18.- Continued.

National Aeronautics and Space Administration
Ames Research Center
Moffett Field, Calif.

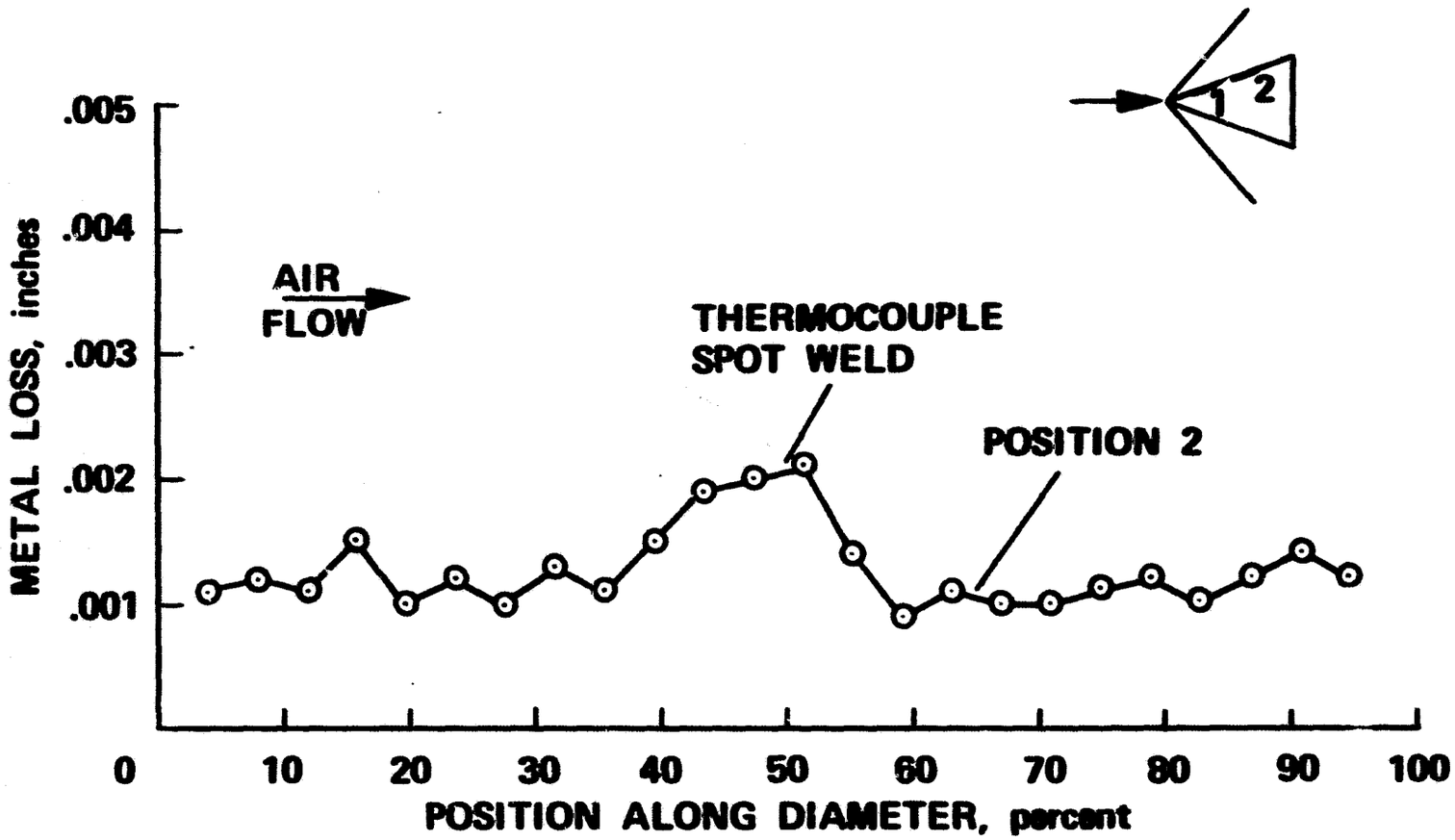

(e) TD-NiCr-7; T = 2000°F, P = 15 Torr.

Figure 18.- Continued.

National Aeronautics and Space Administration
Ames Research Center
Moffett Field, Calif.

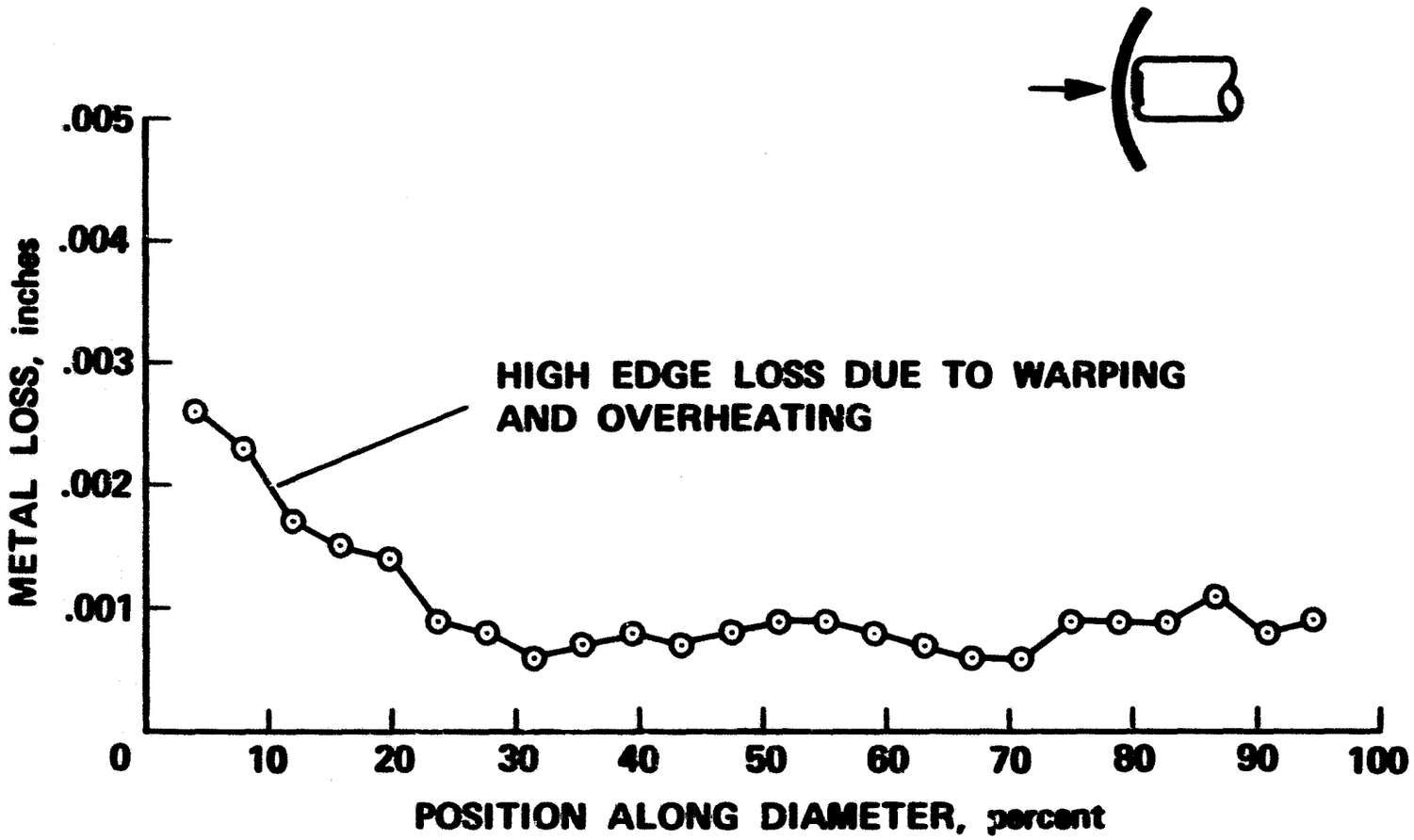

(f) TD-NiCrAlY; T = 2200°F, P = 15 Torr.

Figure 18.- Concluded.

National Aeronautics and Space Administration
Ames Research Center
Moffett Field, Calif.

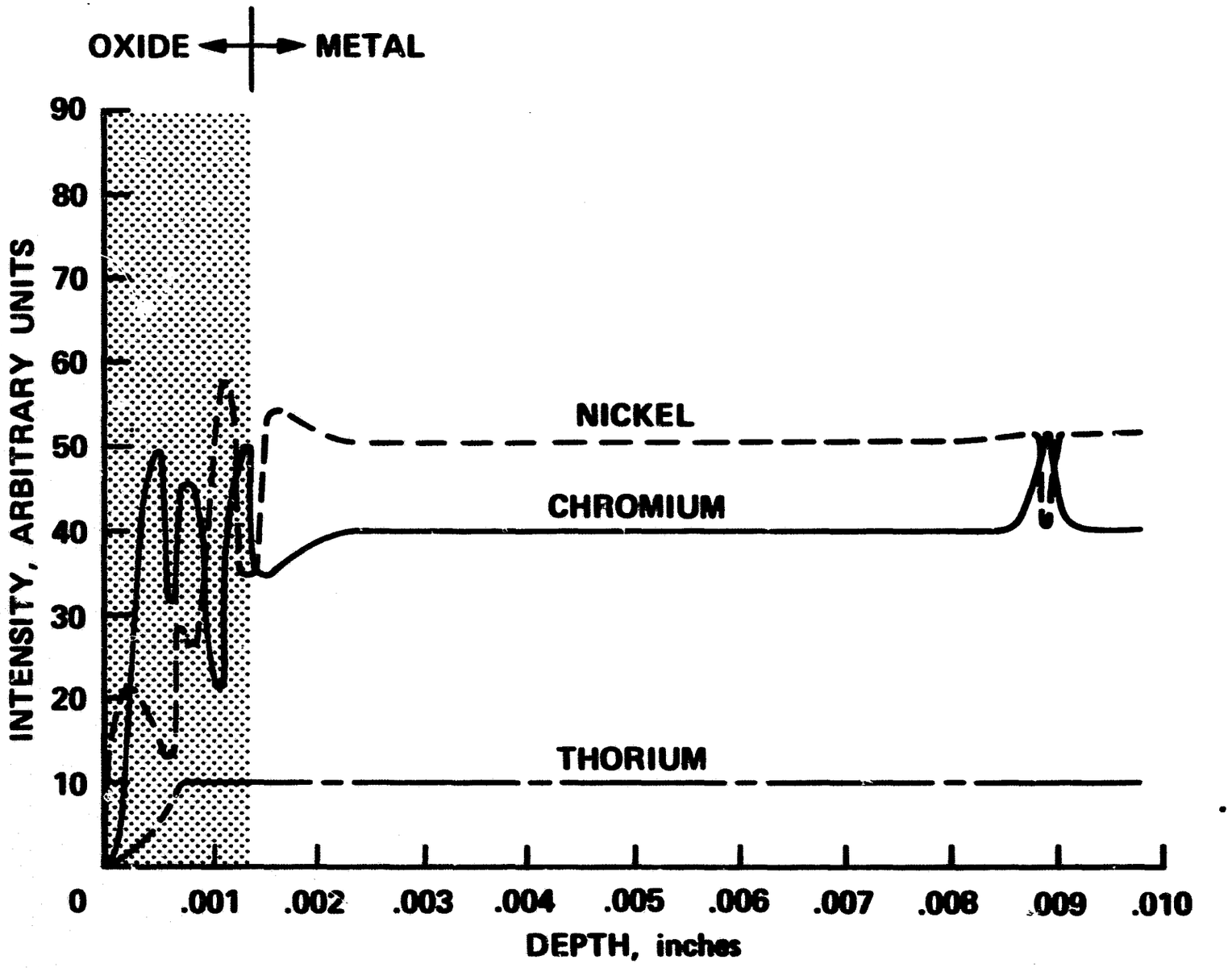

(a) TD-NiCr-1; T = 1800°F, P = 15 Torr.

Figure 19.- Microprobe surveys across sample thickness. Courtesy of Lewis Research Center.

National Aeronautics and Space Administration
Ames Research Center
Moffett Field, Calif.

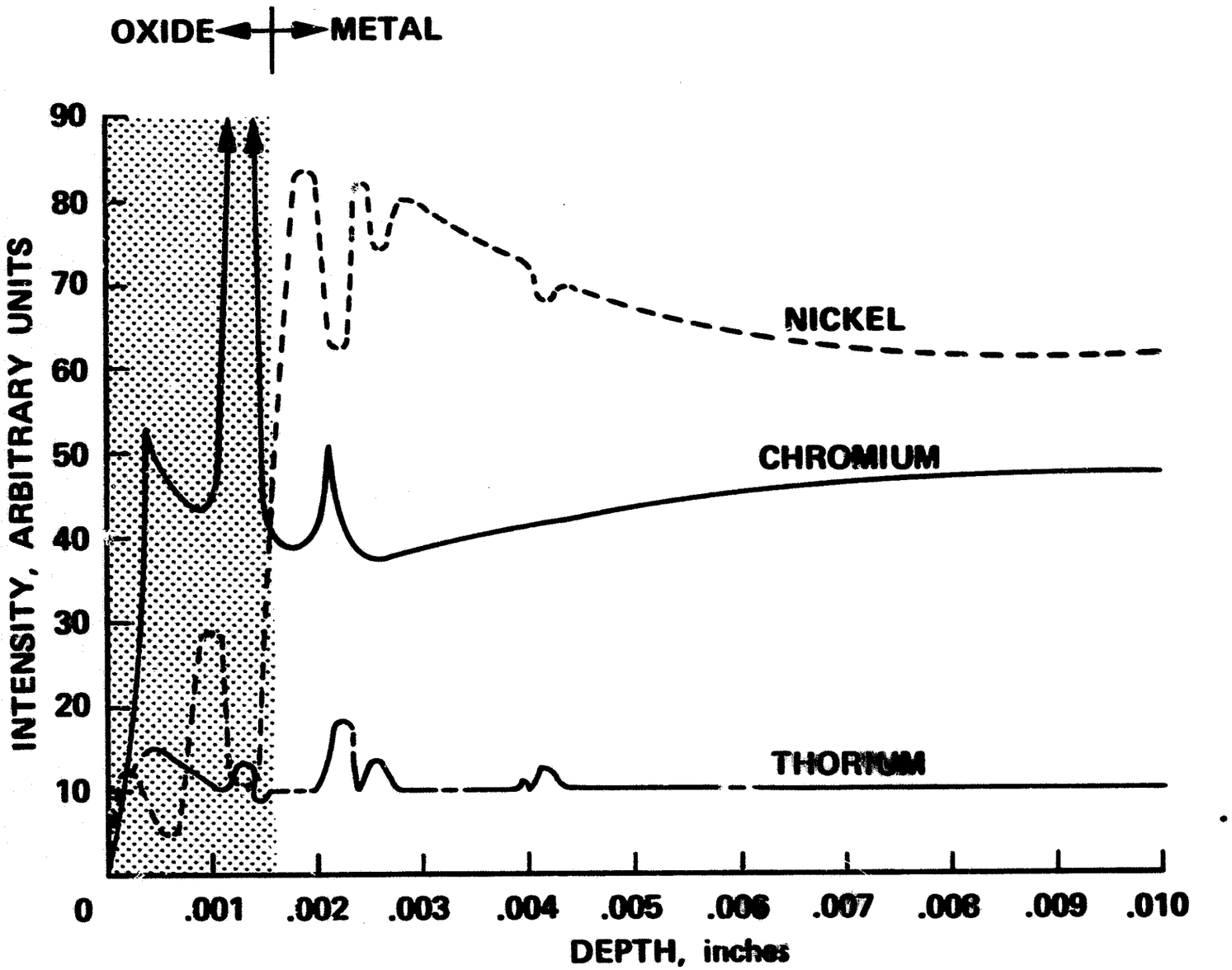

(b) TD-NiCr-2; T = 2200°F, P = 15 Torr.

Figure 19.- Continued.

National Aeronautics and Space Administration
Ames Research Center
Moffett Field, Calif.

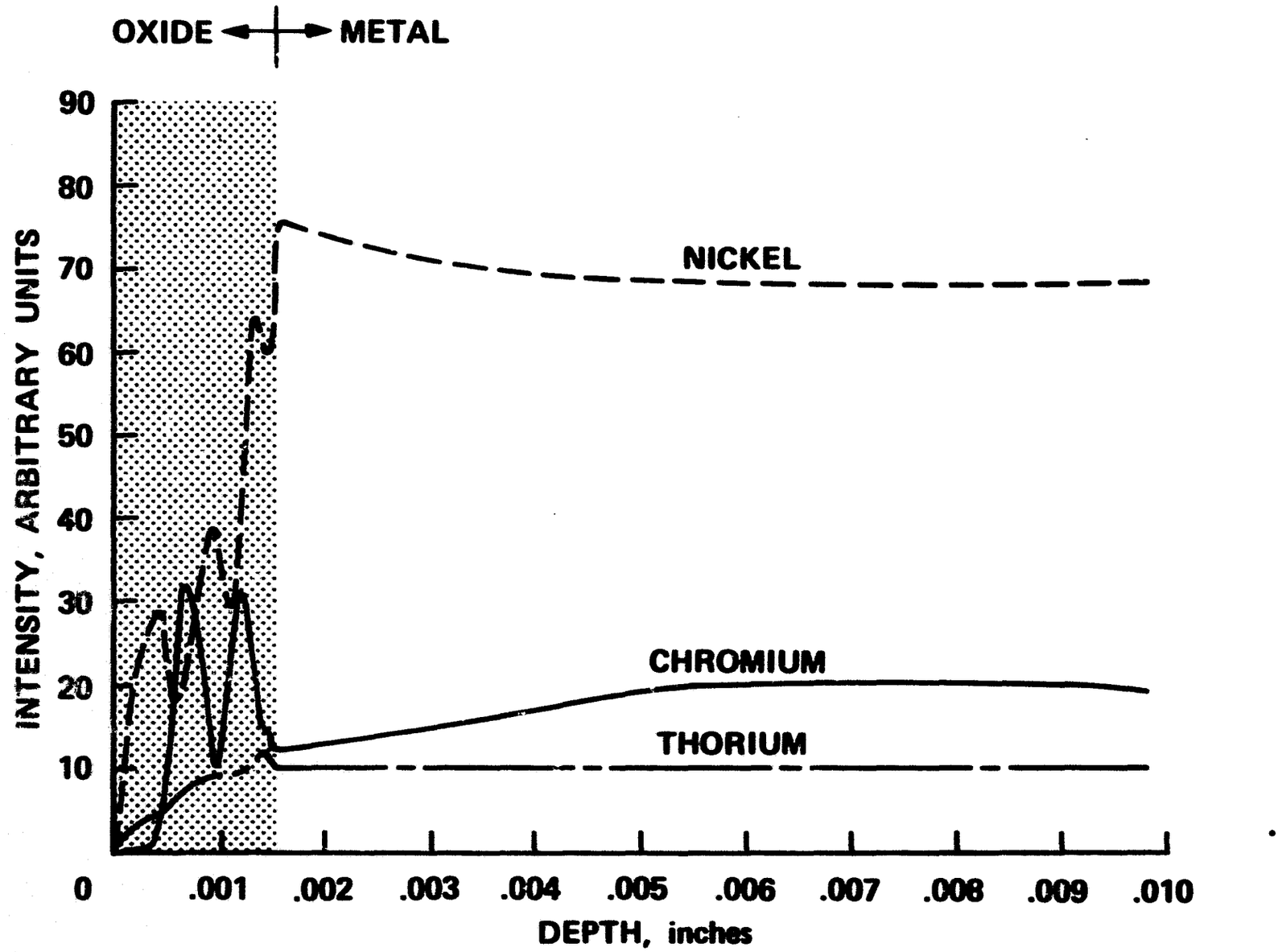

(c) TD-NiCr-8; T = 2200°F, P = 30 Torr.

Figure 19.- Continued.

National Aeronautics and Space Administration
Ames Research Center
Moffett Field, Calif.

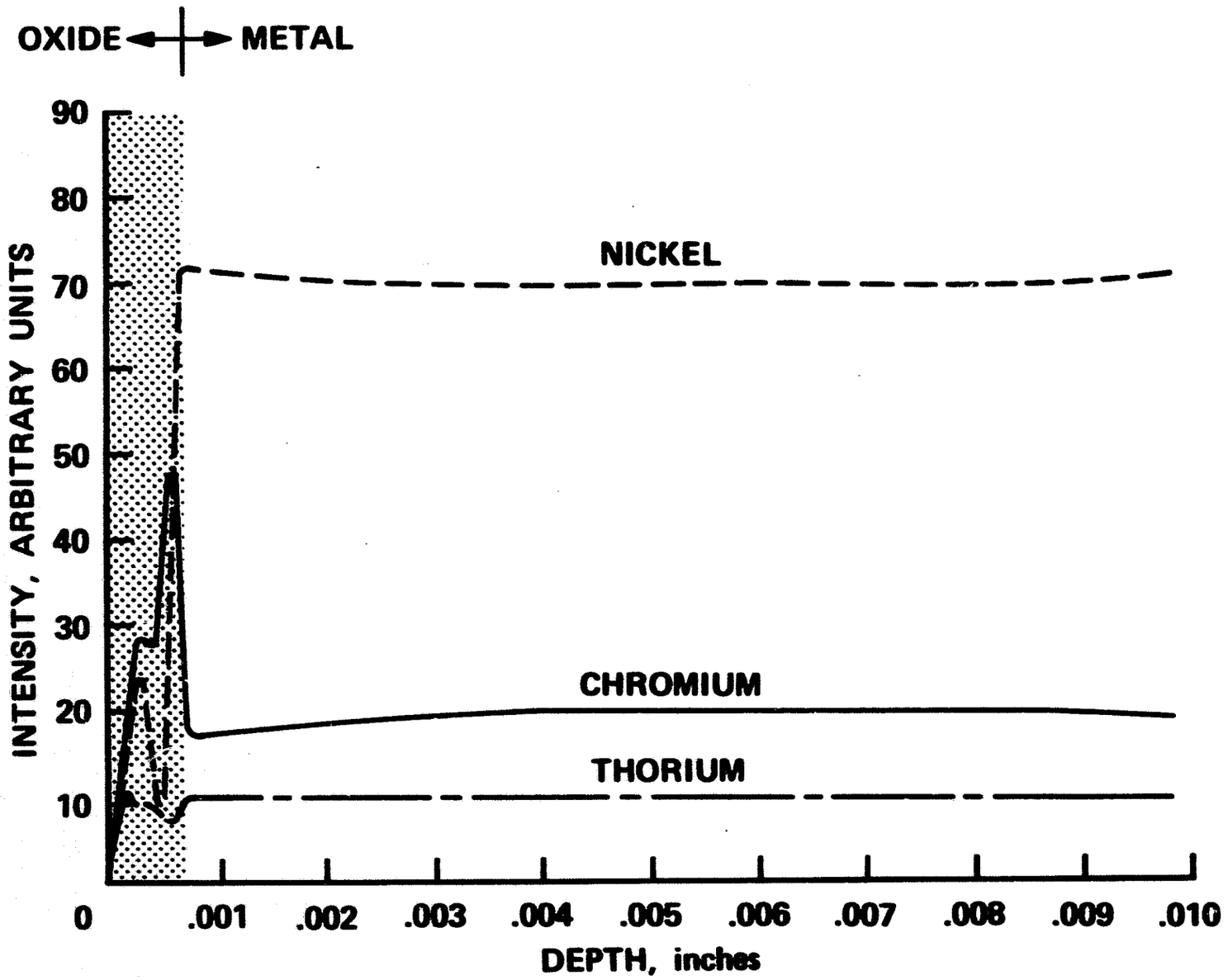

(d) TD-NiCr-6; T = 2200°F, P = 15 Torr.

Figure 19.- Continued.

National Aeronautics and Space Administration
Ames Research Center
Moffett Field, Calif.

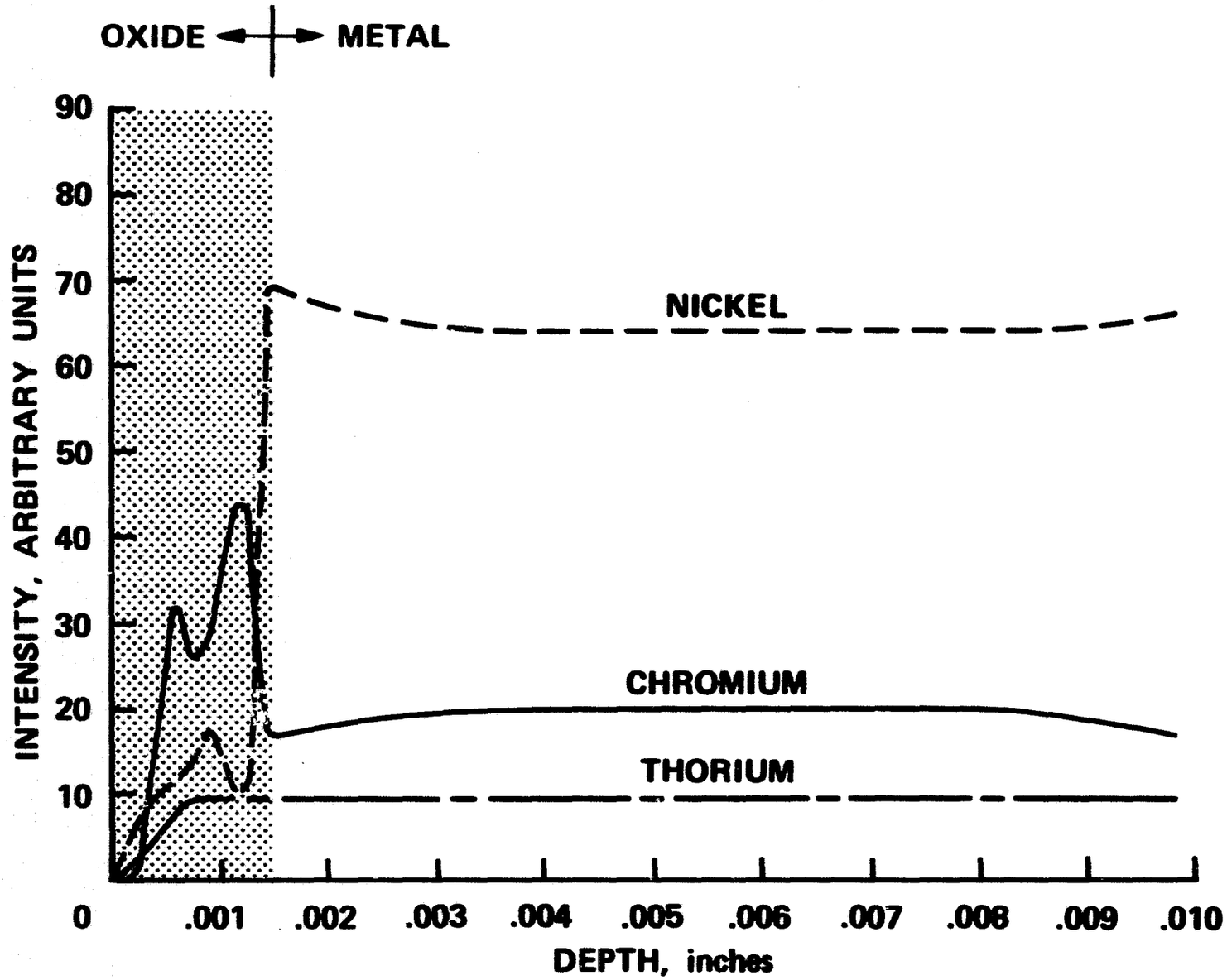

(e) TD-NiCr-7; T = 2000°F, P = 15 Torr.

Figure 19.- Continued.

National Aeronautics and Space Administration
Ames Research Center
Moffett Field, Calif.

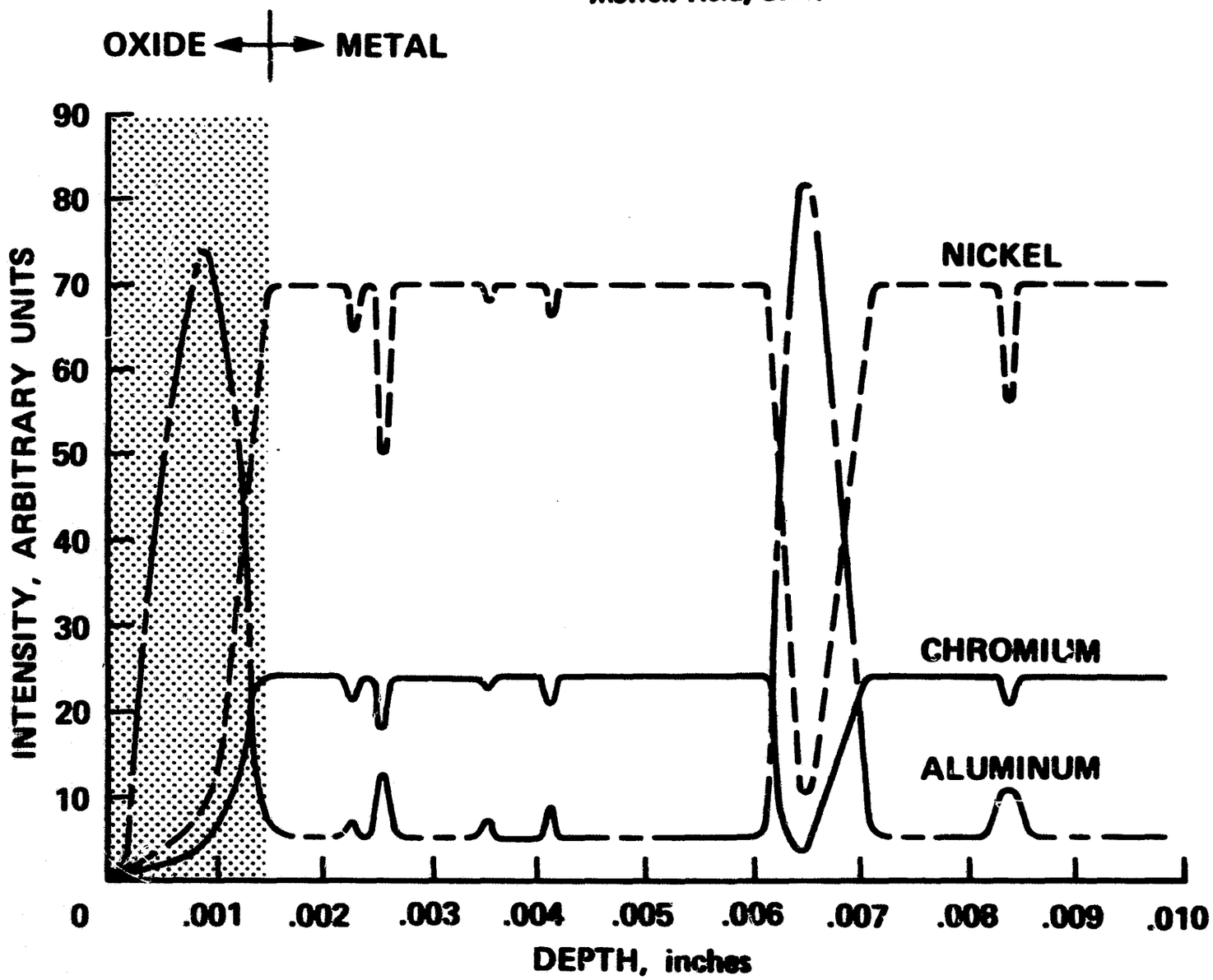

(f) TD-NiCrAlY; T = 2200°F, P = 15 Torr.

Figure 19.- Concluded.